Thermodynamic Model of the System $H^+-NH_4^+-Na^+-SO_4^{2-}-NO_3^--Cl^--H_2O$ at 298.15 K

Simon L. Clegg* and Peter Brimblecombe

School of Environmental Sciences, University of East Anglia, Norwich NR4 7TJ, U.K.

Anthony S. Wexler

Department of Mechanical Engineering, University of Delaware, Newark, Delaware 19716

Received: September 17, 1997; In Final Form: December 2, 1997

A multicomponent mole-fraction-based thermodynamic model of the $H^+-NH_4^+-Na^+-SO_4^{2-}-NO_3^--Cl^--H_2O$ system is used to represent aqueous-phase activities, equilibrium partial pressures (of H_2O, HNO_3, HCl, and NH_3), and saturation with respect to 19 solid phases ($(NH_4)_2SO_{4(cr)}$, $(NH_4)_3H(SO_4)_{2(cr)}$, $NH_4HSO_{4(cr)}$, $NH_4NO_{3(cr)}$, $NH_4Cl_{(cr)}$, $Na_2SO_4{\cdot}10H_2O_{(cr)}$, $Na_2SO_{4(cr)}$, $Na_3H(SO_4)_{2(cr)}$, $NaHSO_4{\cdot}H_2O_{(cr)}$, $NaHSO_{4(cr)}$, $NaH_3(SO_4)_2{\cdot}H_2O_{(cr)}$, $NaNO_{3(cr)}$, $NaCl_{(cr)}$, $NH_4HSO_4{\cdot}NH_4NO_{3(cr)}$, $(NH_4)_2SO_4{\cdot}2NH_4NO_{3(cr)}$, $(NH_4)_2SO_4{\cdot}3NH_4NO_{3(cr)}$, $(NH_4)_2SO_4{\cdot}Na_2SO_4{\cdot}4H_2O_{(cr)}$, $Na_2SO_4{\cdot}NaNO_3{\cdot}H_2O_{(cr)}$, $2NaNO_3{\cdot}NH_4NO_{3(cr)}$). The model is valid for concentrations from infinite dilution to saturation (with respect to the solid phases) and to about 40 mol kg^{-1} for acid sulfate systems which can remain liquid to concentrations approaching the pure acid. Parameters for $H_2SO_4-H_2O$ interactions were adopted from a previous study, and values for other binary (water−electrolyte) and ternary (water and three ions) interactions were determined from extensive literature data for salt solubilities, electromotive forces, osmotic coefficients, and vapor pressures. The model is compared with solubility measurements for the quaternary ion systems $H^+-Na^+-SO_4^{2-}-Cl^--H_2O$ and $NH_4^+-Na^+-SO_4^{2-}-Cl^--H_2O$.

1. Introduction

Acid ammonium sulfate aerosols, with additions of nitrate and sea salt, are ubiquitous in the lower troposphere.[1−3] They are an important influence on urban air quality, for example in the Los Angeles basin,[4] and there have been numerous chemical modeling studies of such aerosols over the past decade and more.[5,6] Mixing rules such as that of Meissner and Kusik[7] have generally been used to estimate ion and solvent activities in aqueous aerosols, as the presence of highly soluble ammonium salts and acid sulfates enables very high aqueous concentrations to be attained at low relative humidity. These concentrations are too great to allow the application of potentially more accurate methods of calculating activities, such as the ion interaction model of Pitzer,[8,9] which has been widely used in brine chemistry.[10] However, many of the concentration limitations of the molality-based ion interaction model are overcome by the Pitzer, Simonson, and Clegg (PSC) approach,[11,12] which has the advantages over mixing rules that associated ionic species and ternary interactions between ions can be treated explicitly. This is important, for example, for modeling the effects of bisulfate formation in acidic sulfate solutions.

In the accompanying publication (hereafter referred to as paper 1) Clegg et al.[13] apply the mole-fraction-based PSC model to the system $H^+-NH_4^+-SO_4^{2-}-NO_3^--H_2O$ to high supersaturation (low relative humidity) and temperatures up to 330 K. This system of equations has also been used to predict the behavior of low-temperature acid solutions related to stratospheric aerosols.[14]

A comprehensive model of inorganic tropospheric aerosols should predict activities, partial pressures, and salt solubilities in $H^+-NH_4^+-Na^+-SO_4^{2-}-NO_3^--Cl^--H_2O$ mixtures over a wide range of temperature. The addition of the ions Na^+ and Cl^- (to the system in paper 1) allows calculations to be carried out for aerosols containing a sea salt component, though omitting Mg^{2+} (present at about one-ninth the concentration of Na^+ in seawater) and other minor constituents. Aqueous solutions of composition $H^+-NH_4^+-Na^+-SO_4^{2-}-NO_3^--Cl^--H_2O$ have the potential to form seven acid sulfate or double salts at 298.15 K in addition to those discussed in paper 1. Equilibrium constants for the formation of several of these are poorly known, as estimates of their values require a knowledge of the activity coefficients of the constituent ions in the concentrated solution mixtures in which they form. Ideally, the properties of supersaturated solutions should also be represented by models intended for atmospheric applications, as aerosols are believed to occur in this state.[15] However, data for supersaturated solutions, especially mixtures, are far from comprehensive even at 298.15 K.

In previous studies we have successfully applied the PSC equations to the systems $H^+-NH_4^+-SO_4^{2-}-H_2O$ and $Na^+-SO_4^{2-}-NO_3^--Cl^--H_2O$ at 298.15 K, including data for supersaturated solutions,[16,17] although there remain difficulties in representing accurately the thermodynamic properties of some electrolytes, particularly aqueous Na_2SO_4, at extreme concentration. These may need to be overcome by refinements in the model equations or by assuming the formation of species such as ion pairs in solution. This is reasonable given often small amounts of water available for hydration of the ions in supersaturated solutions, but represents a complicating factor as there are few data with which the concentrations of such species can be directly constrained.

In this work we present a model of the full $H^+-NH_4^+-Na^+-SO_4^{2-}-NO_3^--Cl^--H_2O$ system at 298.15 K, restricted to subsaturated and saturated solutions. The purpose of this model

S1089-5639(97)03043-0 CCC: $15.00
Published on Web 02/27/1998

is (1) to determine equilibrium constants of acid sulfate salts and other double salts that form in solution mixtures and provide a more accurate method of exploring phase equilibrium relationships for these inorganic aerosols than has hitherto been available; (2) to establish the basis for a temperature-dependent model for solutions up to saturation with respect to dissolved salts; and (3) to provide a reference to aid comparisons between different methods of estimating activity coefficients used in aerosol models. It will also allow the requirements for accuracy in the thermodynamic calculations to be assessed relative to uncertainties in aerosol composition, atmospheric conditions (temperature, relative humidity, and the partial pressures of soluble gases), and physical transport processes in typical atmospheric modeling applications. For these purposes the parameterization of the activity coefficient equations for each component electrolyte has been limited to a maximum concentration within which the available measurements are represented to within, or close to, experimental precision. For all salts this is at or above the concentration at which each binary solution becomes saturated. The model should provide a more accurate method of predicting the properties of the system at 298.15 K (principally HNO_3, HCl, NH_3, and H_2O partial pressures and solid/liquid phase equilibrium) than currently available. It is validated by comparisons with measured salt solubilities in two quaternary ion systems.

2. Theory

In the model, all liquid-phase concentrations and activity coefficients are expressed on the mole fraction scale. The mole fraction x_i of species i is given by $x_i = n_i/(\sum_j n_j)$, where n_i is the number of moles of component i and the summation j is over all solution components including the solvent. The activities a_i of all components i are given by $a_i = f_i x_i$ where f_i is the activity coefficient. The reference state for the activity coefficients of solute species is one of infinite dilution with respect to the solvent, identified by subscript 1, and activity coefficients on this basis are denoted f_i^*; thus $f_i^* \rightarrow 1$ as $x_1 \rightarrow 1$. The reference state for the activity coefficient of the pure solvent is the pure liquid, so that $f_1 \rightarrow 1$ as $x_1 \rightarrow 1$. The relationship between mole fraction and molality-based activity coefficients and equilibrium constants, and definitions of molal (ϕ) and rational (g) osmotic coefficients, are given in eqs 2−4 of paper (1).

The present model is similar to that in paper (1) in that conventional strong electrolytes are treated as fully dissociated in solution, but the dissociation of the bisulfate ion (HSO_4^-) is considered explicitly (eq 5 and eq 6 of paper 1).

Equilibrium expressions for the formation of solid phases, and for vapor−liquid equilibrium, are the same as those given in paper (1), and are summarized below.

2.1. Formation of Solid Phases. For a salt $M_{\nu+}X_{\nu-}\cdot zH_2O_{(cr)}$ in equilibrium with an aqueous solution containing cation M and anion X,

$$M_{\nu+}X_{\nu-}\cdot zH_2O_{(cr)} \rightleftharpoons \nu_+ M_{(aq)} + \nu_- X_{(aq)} + zH_2O_{(l)} \quad (1a)$$

$${}^xK_S = aM^{\nu+}aX^{\nu-}a_1{}^z/a(M_{\nu+}X_{\nu-}\cdot zH_2O_{(cr)}) \quad (1b)$$

where $aM^{\nu+}$ and $aX^{\nu-}$ are the mole fraction activities of M and X, and a_1 is the water activity. Because the activity of the pure solid phase $a(M_{\nu+}X_{\nu-}\cdot zH_2O_{(cr)})$ is by definition unity, only the activity product of the ions and solvent in eq 1b is significant. Solubility data for all the systems studied have been used to constrain the model, and values of the equilibrium constants themselves, consistent with the modeled activities, have also been determined here.

2.2. Vapor−Liquid Equilibrium. The solubilities of the volatile acids HNO_3 and HCl in aqueous solution are expressed as the equilibrium

$$HX_{(g)} \rightleftharpoons H^+_{(aq)} + X^-_{(aq)} \quad (2a)$$

$${}^xK_H = xH^+ f_H^* xX^- f_X^*/pHX \quad (2b)$$

where pHX (atm) is the partial pressure of acid gas HX. (For conversion to SI units, atm = 101 325 Pa.) The Henry's law constants of HNO_3 and HCl are 853.1 and 662.1 atm^{-1}, respectively, at 298.15 K.[14,18]

The solubility of NH_3 is described in terms of the equilibrium between the gas-phase molecule and aqueous H^+ and NH_4^+ ions:

$$NH_{3(g)} + H^+_{(aq)} \rightleftharpoons NH_4{}^+_{(aq)} \quad (3a)$$

$${}^x\boldsymbol{K}'_H = xNH_4{}^+ f_{NH_4}{}^*/(xH^+ f_H^* pNH_3) \quad (3b)$$

where ${}^x\boldsymbol{K}'_H$ (atm^{-1}) is equivalent to the "conventional" Henry's law constant for NH_3 (K'_H, for $NH_{3(g)} \rightleftharpoons NH_{3(aq)}$) divided by the acid dissociation constant of NH_4^+ (K_a, for $NH_4{}^+_{(aq)} \rightleftharpoons H^+_{(aq)} + NH_{3(aq)}$). At 298.15 K, ${}^x\boldsymbol{K}'_H$ is equal to 1.066×10^{11} atm^{-1}.[19,20]

2.3. The Model. Equations for solute and solvent activity coefficients in a liquid mixture are presented in general form by Clegg et al.,[12] and are given for the case of a single solute in water in paper 1.

The model contains interaction parameters whose values must be determined from empirical data. For a single ionic solute $M_{\nu+}X_{\nu-}$ in water there are parameters B_{MX}, $W_{1,MX}$, $U_{1,MX}$, and $V_{1,MX}$ that account for interactions between the solvent and ions M and X. The cation−anion coefficients α_{MX} may either be set to fixed values or, where necessary, fitted together with the parameters for solvent−cation−anion interactions noted above.

In multicomponent solutions based on a single solvent and containing several cations and anions, there also arise mixture parameters of type $W_{ii'j}$, $Q_{1,ii'j}$ and $U_{ii'j}$, where i and i' are dissimilar cations or anions and j is an ion of opposite sign. These have the greatest influence in very concentrated solutions and are typically determined from vapor pressures, electromotive forces (emfs), or salt solubilities for three-ion mixtures.

The determination of parameter values for pure (single-solute) aqueous solutions and mixtures is summarized in the following section.

3. Parameterization of the Model

The present model does not, in general, extend to supersaturated solutions. However, it represents the thermodynamic properties of aqueous mixtures up to, and including, saturation with respect to nineteen possible solid phases at 298.15 K. Parameterization of the model over such a restricted range of concentrations leads to an increase in accuracy at low to moderate concentration compared, for example, to the extended fits of Clegg et al.[17]

Figure 1 shows the relationship between water activity (relative humidity) and concentration for each of the binary solutions, in most cases up to the saturation molality. There is a wide diversity of behavior. For example, 25 mol kg^{-1} solutions of NH_4NO_3 and H_2SO_4 are in equilibrium with relative

TABLE 1: Fitted Binary Model Parameters for the System $H^+-NH_4^+-Na^+-SO_4^{2-}-NO_3^--Cl^--H_2O$ at 298.15 K[a]

parameter	value		parameter	value		parameter	value	
$B_{H\cdot NO3}$	13.5342	a	$B_{H\cdot Cl}$	4.65969	e	$B_{NH4\cdot HSO4}$	14.2262	h
$\alpha_{H\cdot NO3}$	17.0	a	$\alpha_{H\cdot Cl}$	15.0	e	$\alpha_{NH4\cdot HSO4}$	19.0	h
$W_{1,H\cdot NO3}$	−3.07186	a	$W_{1,H\cdot Cl}$	−0.568291	e	$W_{1,NH4\cdot HSO4}$	−2.56359	h
$U_{1,H\cdot NO3}$	1.96582	a	$U_{1,H\cdot Cl}$	2.07244	e	$U_{1,NH4\cdot HSO4}$	−0.796274	h
$V_{1,H\cdot NO3}$	−1.41191	a	$V_{1,H\cdot Cl}$	−1.25000	e	$V_{1,NH4\cdot HSO4}$	0.663585	h
$B_{NH4\cdot SO4}$	−2.858988	b	$B_{NH4\cdot NO3}$	24.7529	f	$B_{NH4\cdot Cl}$	4.65969	i
$\alpha_{NH4\cdot SO4}$	13.0	b	$\alpha_{NH4\cdot NO3}$	7.0	f	$\alpha_{NH4\cdot Cl}$	15.0	i
$W_{1,NH4\cdot SO4}$	−0.740149	b	$B^1_{NH4\cdot NO3}$	−29.9961	f	$W_{1,NH4\cdot Cl}$	−0.568291	i
$U_{1,NH4\cdot SO4}$	0.940860	b	$\alpha^1_{NH4\cdot NO3}$	13.0	f	$U_{1,NH4\cdot Cl}$	2.07244	i
$V_{1,NH4\cdot SO4}$	−2.587430	b	$W_{1,NH4\cdot NO3}$	0.900729	f	$V_{1,NH4\cdot Cl}$	−1.25000	i
			$U_{1,NH4\cdot NO3}$	0.379736	f			
$B_{Na\cdot HSO4}$	62.27961	c	$V_{1,NH4\cdot NO3}$	−1.42646	f	$B_{Na\cdot NO3}$	26.9994	j
$\alpha_{Na\cdot HSO4}$	19.0	c				$\alpha_{Na\cdot NO3}$	5.0	j
$W_{1,Na\cdot HSO4}$	−2.932425	c	$B_{Na\cdot SO4}$	34.4660	g	$B^1_{Na\cdot NO3}$	-21.6050	j
$U_{1,Na\cdot HSO4}$	−4.857197	c	$\alpha_{Na\cdot SO4}$	13.0	g	$\alpha^1_{Na\cdot NO3}$	13.0	j
$V_{1,Na\cdot HSO4}$	4.888311	c	$W_{1,Na\cdot SO4}$	−3.72596	g	$W_{1,Na\cdot NO3}$	0.0526908	j
			$U_{1,Na\cdot SO4}$	−1.95916	g	$U_{1,Na\cdot NO3}$	0.266644	j
$B_{Na\cdot Cl}$	19.9338	d	$V_{1,Na\cdot SO4}$	−4.86057	g	$V_{1,Na\cdot NO3}$	−2.30288	j
$\alpha_{Na\cdot Cl}$	5.0	d						
$W_{1,Na\cdot Cl}$	−5.64608	d						
$U_{1,Na\cdot Cl}$	−3.60925	d						
$V_{1,Na\cdot Cl}$	−2.45982	d						

[a] Parameters for $H^+-HSO_4^--SO_4^{2-}-H_2O$ (aqueous H_2SO_4) interactions are given by Clegg and Brimblecombe.[21] The interaction parameters above were determined from data for the following systems: (a) HNO_3-H_2O; (b) $(NH_4)_2SO_4-H_2O$; (c) $Na_2SO_4-H_2SO_4-H_2O$; (d) $NaCl-H_2O$; (e) $HCl-H_2O$; (f) $NH_4NO_3-H_2O$; (g) $Na_2SO_4-H_2O$; (h) $(NH_4)_2SO_4-H_2SO_4-H_2O$; (i) NH_4Cl-H_2O; (j) $NaNO_3-H_2O$.

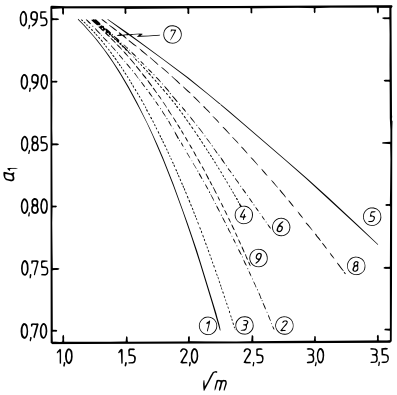

Figure 1. Relationship between water activity (a_1) and molality (m/mol kg^{-1}) for single-solute solutions at 298.15 K. Numbered solutes: (1) $H_2SO_{4(aq)}$; (2) $HNO_{3(aq)}$; (3) $HCl_{(aq)}$; (4) $(NH_4)_2SO_{4(aq)}$; (5) $NH_4NO_{3(aq)}$ (saturation occurs at ∼26 mol kg^{-1}); (6) $NH_4Cl_{(aq)}$; (7) $Na_2SO_{4(aq)}$ (lies between the curves for $(NH_4)_2SO_{4(aq)}$ and $NH_4Cl_{(aq)}$); (8) $NaNO_{3(aq)}$; (9) $NaCl_{(aq)}$.

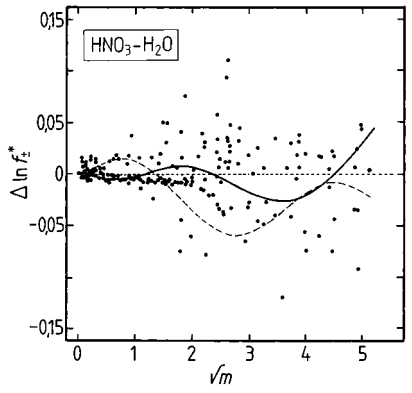

Figure 2. Fit of the model to mean activity coefficients of HNO_3 ($f_\pm$*) in $HNO_{3(aq)}$ at 298.15 K, plotted against the square root of molality (m/mol kg^{-1}). Symbols: dots, Clegg and Brimblecombe[18] (evaluated data from many sources). Lines: solid, model of Carslaw et al.;[14] dashed, equation of Hamer and Wu.[22]

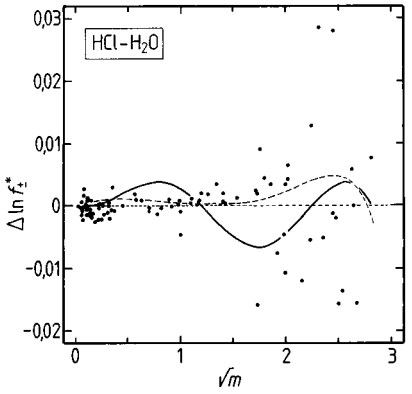

Figure 3. Fit of the model to mean activity coefficients of HCl ($f_\pm$*) in $HCl_{(aq)}$ at 298.15 K, plotted against the square root of molality (m/mol kg^{-1}). Symbols: dots, Carslaw et al.[14] (evaluated data from many sources). Lines: solid, model of Carslaw et al.;[14] dashed, equation of Hamer and Wu.[22]

humidities of 62% and only 4%, respectively. The amounts of water taken up by atmospheric aerosols are thus highly dependent upon composition, especially at low relative humidities where the curves for the individual electrolytes in Figure 1 diverge.

In the following subsections, the parameterization of each binary and ternary system is summarized. All model parameters are listed in Tables 1 and 2, and equilibrium constants for the formation of solid phases in Table 3. For aqueous mixtures that have been modeled in previous studies, for example in paper 1, fits of the present model to the available data are generally not shown here. In other cases they are given in Figures 24−42, with summary diagrams contained in the main text. The quantities $\Delta\phi$ and $\Delta f_\pm$*, shown in Figures 2−9, are differences between the experimental and fitted values of the osmotic and mean activity coefficient, respectively.

3.1. $H_2SO_4-H_2O$, HNO_3-H_2O, and $HCl-H_2O$. For aqueous H_2SO_4 the parameterization of Clegg and Brimblecombe[21] is used, as for the model in paper 1, to represent activity and osmotic coefficients to 40 mol kg^{-1} (a relative humidity of 0.59%). For HNO_3-H_2O, critically evaluated activity data

TABLE 2: Fitted Ternary Model Parameters for the System $H^+-NH_4^+-Na^+-SO_4^{2-}-NO_3^--Cl^--H_2O$ at 298.15 K[a]

parameter	value		parameter	value		parameter	value	
$W_{H\cdot NH4\cdot HSO4}$	−19.494	h	$W_{H\cdot Na\cdot Cl}$	2.2490	n	$W_{HSO4\cdot NO3\cdot NH4}$	−2.7465	s
$Q_{1,H\cdot NH4\cdot HSO4}$	8.7607	h	$Q_{1,H\cdot Na\cdot Cl}$	−0.25080	n			
						$Q_{1,SO4\cdot NO3\cdot NH4}$	2.9795	t
$W_{H\cdot NH4\cdot SO4}$	−4.3507	h	$W_{NH4\cdot Na\cdot SO4}$	−1.4832	o	$U_{SO4\cdot NO3\cdot NH4}$	−1.2163	t
$U_{H\cdot NH4\cdot SO4}$	6.5216	h	$Q_{1,NH4\cdot Na\cdot SO4}$	0.76211	o			
						$W_{SO4\cdot NO3\cdot Na}$	−9.498	u
$W_{H\cdot NH4\cdot NO3}$	−3.0708	k	$W_{NH4\cdot Na\cdot NO3}$	−0.35411	p	$Q_{1\cdot SO4\cdot NO3\cdot Na}$	8.528	u
$Q_{1,H\cdot NH4\cdot NO3}$	0.28491	k	$Q_{1,NH4\cdot Na\cdot NO3}$	0.046254	p			
$U_{H\cdot NH4\cdot NO3}$	−0.46338	k	$U_{NH4\cdot Na\cdot NO3}$	0.2130	p	$U_{SO4\cdot Cl\cdot NH4}$	−1.0709	v
						$Q_{1,SO4\cdot Cl\cdot NH4}$	1.0869	v
$W_{H\cdot NH4\cdot Cl}$	−19.977	l	$W_{NH4\cdot Na\cdot Cl}$	−5.6414	q			
$Q_{1,H\cdot NH4\cdot Cl}$	10.233	l	$Q_{1,NH4\cdot Na\cdot Cl}$	3.2919	q	$W_{SO4\cdot Cl\cdot Na}$	4.827	w
						$Q_{1\cdot SO4\cdot Cl\cdot Na}$	0.05163	w
$W_{H\cdot Na\cdot HSO4}$	−8.96894	c	$W_{HSO4\cdot SO4\cdot NH4}$	−14.753	h			
$Q_{1,H\cdot Na\cdot HSO4}$	4.16202	c	$Q_{1,HSO4\cdot SO4\cdot NH4}$	4.7204	h	$W_{NO3\cdot Cl\cdot NH4}$	−0.2207	x
$U_{H\cdot Na\cdot HSO4}$	−2.92819	c	$U_{HSO4\cdot SO4\cdot NH4}$	−16.317	h	$Q_{1,NO3\cdot Cl\cdot NH4}$	−0.1173	x
$W_{H\cdot Na\cdot SO4}$	15.9075	c						
$Q_{1,H\cdot Na\cdot SO4}$	−8.82425	c	$Q_{1,HSO4\cdot SO4\cdot Na}$	−4.68641	c	$W_{NO3\cdot Cl\cdot Na}$	−6.923	y
						$Q_{1\cdot NO3\cdot Cl\cdot Na}$	4.181	y
			$W_{HSO4\cdot NO3\cdot H}$	−4.280	r			
$W_{H\cdot Na\cdot NO3}$	0.46039	m	$U_{HSO4\cdot NO3\cdot H}$	2.3221	r			
$U_{H\cdot Na\cdot NO3}$	1.1749	m	$W_{SO4\cdot NO3\cdot H}$	−0.83228	r			

[a] Parameters $W_{ii'j}$ and $Q_{1,ii'j}$ are symmetrical; thus $W_{i'ij} = W_{ii'j}$ and $Q_{1,i'ij} = Q_{1,ii'j}$. However, $U_{i'ij} = -U_{ii'j}$. The interaction parameters above were determined from data for the following systems: (c) $Na_2SO_4-H_2SO_4-H_2O$; (h) $(NH_4)_2SO_4-H_2SO_4-H_2O$; (k) $HNO_3-NH_4NO_3-H_2O$; (l) $HCl-NH_4Cl-H_2O$; (m) $HNO_3-NaNO_3-H_2O$; (n) $HCl-NaCl-H_2O$; (o) $(NH_4)_2SO_4-Na_2SO_4-H_2O$; (p) $NH_4NO_3-NaNO_3-H_2O$; (q) $NH_4Cl-NaCl-H_2O$; (r) $HNO_3-H_2SO_4-H_2O$; (s) $NH_4HSO_4-NH_4NO_3-H_2O$; (t) $NH_4NO_3-(NH_4)_2SO_4-H_2O$; (u) $NaNO_3-Na_2SO_4-H_2O$; (v) $(NH_4)_2SO_4-NH_4Cl-H_2O$; (w) $(Na)_2SO_4-NaCl-H_2O$; (x) $NH_4NO_3-NH_4Cl-H_2O$; (y) $NaNO_3-NaCl-H_2O$.

TABLE 3: Equilibrium Constants for Solid Phases for the System $H^+-NH_4^+-Na^+-SO_4^{2-}-NO_3^--Cl^--H_2O$ at 298.15 K

solid phase	$\ln({}^xK_S)$	solid phase	$\ln({}^xK_S)$
$(NH_4)_2SO_4$	−12.01	$NaH_3(SO4)_2\cdot H_2O$	−13.02
$(NH_4)_3H(SO_4)_2$	−26.04	$NaNO_3$	−5.552
NH_4HSO_4	−11.43	NaCl	−4.388
NH_4NO_3	−5.531	$NH_4HSO_4\cdot NH_4NO_3$	−17.49
NH_4Cl	−5.178	$(NH_4)_2SO_4\cdot 2NH_4NO_3$	−23.67
$Na_2SO_4\cdot 10H_2O$	−14.87	$(NH_4)_2SO_4\cdot 3NH_4NO_3$	−29.37
Na_2SO_4	−12.76	$(NH_4)_2SO_4\cdot Na_2SO_4\cdot 4H_2O$	−28.00
$Na_3H(SO_4)_2$	−25.77	$Na_2SO_4\cdot NaNO_3\cdot H_2O$	−19.28
$NaHSO_4\cdot H_2O$	−12.29	$(NH_4NO_3\cdot 2NaNO_3)^a$	−17.11
$NaHSO_4$	−10.65		

[a] This solid may be metastable (see section 3.15); its formation is consistent with the ternary parameters $W_{NH4\cdot Na\cdot NO3} = -0.465\,89$, $Q_{1,NH4\cdot Na\cdot NO3} = 0.137\,47$, and $U_{NH4\cdot Na\cdot NO3} = 0.228\,11$, which should be substituted for the values in Table 1.

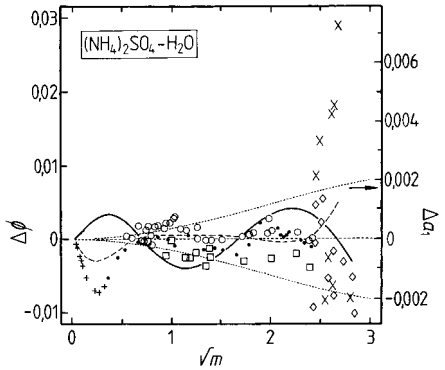

Figure 4. Fit of the model to molal osmotic coefficients of $(NH_4)_2SO_{4(aq)}$ (ϕ, left-hand scale) at 298.15 K, plotted against the square root of molality (m/mol kg^{-1}). Symbols: dots, Wishaw and Stokes;[56] pluses, Goldberg;[57] open circles, Palmer and Milioto;[58] open squares, Filippov et al.;[59] open diamonds, Tang and Munkelwitz;[59] crosses, Clegg et al.[23] Lines: solid, model 1;[23] dashed, model of Clegg et al.;[58] dotted, changes in water activity (Δa_1, right-hand scale) for an error in the osmotic coefficient of ±0.01.

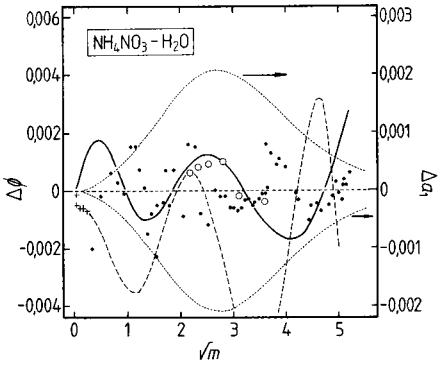

Figure 5. Fit of the model to molal osmotic coefficients of $NH_4NO_{3(aq)}$ (ϕ, left-hand scale) at 298.15 K, plotted against the square root of molality (m/mol kg^{-1}). Symbols: dots, Wishaw and Stokes;[60] pluses, Hamer and Wu;[22] open circles, Kirgintsev and Luk'yanov.[47] Lines: solid, model 1; dashed, equation of Hamer and Wu;[22] dotted, changes in water activity (Δa_1, right-hand scale) for an error in the osmotic coefficient of ±0.01.

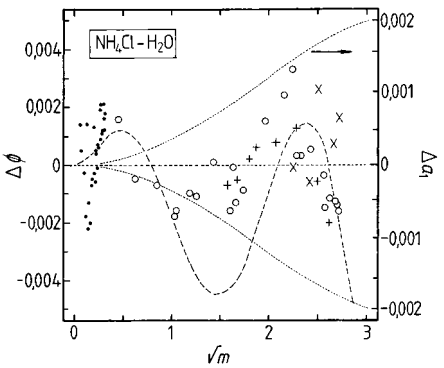

Figure 6. Fit of the model to molal osmotic coefficients of $NH_4Cl_{(aq)}$ (ϕ) at 298.15 K, plotted against the square root of molality (m/mol kg^{-1}). Symbols: dots, Garnsey and Prue;[61] open circles, Wishaw and Stokes;[60] pluses, Kirgintsev and Luk'yanov;[62] crosses, Shul'ts et al.[63] Lines: dashed, equation of Hamer and Wu;[22] dotted, changes in water activity (Δa_1, right-hand scale) for an error in the osmotic coefficient of ±0.01.

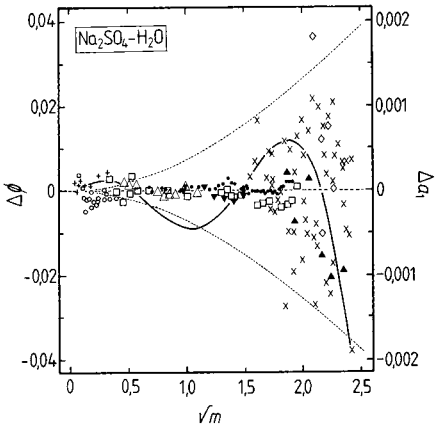

Figure 7. Fit of the model to molal osmotic coefficients of $Na_2SO_{4(aq)}$ (ϕ) at 298.15 K, plotted against the square root of molality (m/mol kg^{-1}). Symbols: dots, Rard and Miller;[64] open circles, Indelli;[65] open squares, Platford;[66] open triangles, Downes and Pitzer;[67] pluses, Randall and Scott;[68] solid inverted triangles, Gibson and Adams;[69] open diamonds, Chan et al.[24] (dynamic experiments); solid triangles, Chan et al.[24] (static experiments); crosses, Tang and Munkelwitz.[70] Lines: solid, model of Clegg et al.;[17] dotted, changes in water activity (Δa_1, right-hand scale) for an error in the osmotic coefficient of ± 0.01.

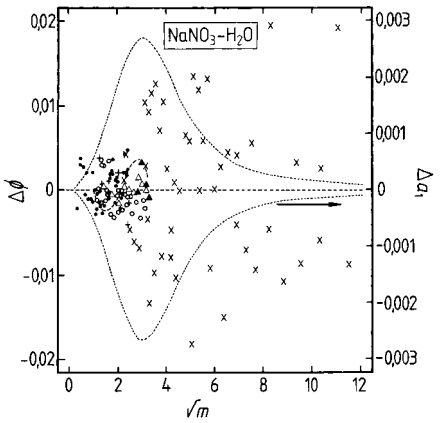

Figure 8. Fit of the model to molal osmotic coefficients of $NaNO_{3(aq)}$ (ϕ) at 298.15 K, plotted against the square root of molality (m/mol kg^{-1}). Symbols: dots, Robinson;[25] open circles, Kirgintsev and Luk'yanov;[71,62] pluses, Bezboruah et al.;[26] open triangles, Kangro and Groeneveld;[72] solid triangles, Pearce and Hopson;[73] crosses, Tang and Munkelwitz.[70] Lines: dashed, evaluation of Wu and Hamer;[74] dotted, changes in water activity (Δa_1, right-hand scale) for an error in the osmotic coefficient of ± 0.01.

(Clegg and Brimblecombe,[18] see their Table 1) are fitted using the mole fraction equations (eq 14 of paper 1) up to a mole fraction ionic strength (I_x) of 0.5, equivalent to 27.5 mol kg^{-1}. Figure 2 shows that the data are represented to within experimental precision, with an improvement in accuracy compared to both the extended fit of Carslaw et al.[14] and the earlier compilation of Hamer and Wu.[22]

Sources of thermodynamic data for aqueous HCl are listed in Table 7 of Carslaw et al.[14] For this model the representation of osmotic and activity coefficients of the pure aqueous acid is limited to 8 mol kg^{-1}, and the fit is shown in Figure 3. Although the data (electromotive force measurements) are quite scattered above about 2.5 mol kg^{-1}, it is clear that the present model better represents the mean activity coefficients of HCl within the fitted range than the 0−20 mol kg^{-1} fit of Carslaw et al.,[14] which was obtained chiefly in order to predict HCl solubilities in highly acidic solutions at stratospheric temperatures.

3.2. $(NH_4)_2SO_4-H_2O$. Available thermodynamic data for this system are listed in Table 4 and consist of isopiestic and

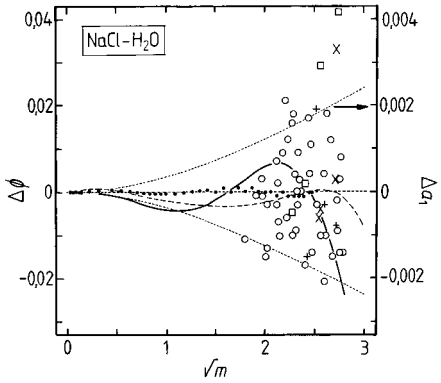

Figure 9. Fit of the model to molal osmotic coefficients of $NaCl_{(aq)}$ (ϕ) at 298.15 K, plotted against the square root of molality (m/mol kg^{-1}). Symbols: dots, critical evaluation of Archer;[27] open circles, Tang et al.;[28] open squares, Chan et al.[24] (static experiments); crosses, Chan et al.[24] (dynamic experiments); pluses, Cohen.[29] Lines: solid, model of Clegg et al.;[17] dashed, equation of Hamer and Wu;[22] dotted, changes in water activity (Δa_1, right-hand scale) for an error in the osmotic coefficient of ± 0.01.

TABLE 4: Sources of Activity Data at 298.15 K for $(NH_4)_2SO_4-H_2O$ Solutions[a]

m^b				
min	max	used[c]	data type[d]	source
0.129	5.830	yes	iso	Wishaw and Stokes[56]
0.583	5.714	yes	iso	Filippov et al.[59]
1.756	2.697	no	iso	Frolov and Nasonova[91]
0.244	5.175	yes	iso	Clegg et al.[58]
4.746	28.193	yes	edb	Clegg et al.[23]
2.868	29.595	yes	edb[e]	Tang and Munkelwitz[70]

[a] As in previous work,[58] osmotic coefficients of aqueous K_2SO_4[57] were used to constrain the model below 0.1 mol kg^{-1}. [b] Molality. [c] Used in the fit of the model. [d] Type of measurement: iso, isopiestic measurement; edb, electrodynamic balance measurements of the water activity/concentration relationship for supersaturated solutions. [e] Data restandardized using osmotic coefficients for subsaturated solutions.

balance (edb) measurements carried out by several different groups. Here, the maximum molality of fit was restricted to 8 mol kg^{-1} (about 2 mol kg^{-1} above the saturation concentration), and the result is shown in Figure 4. There is an improvement in accuracy over the extended fit of Clegg et al.,[23] used for the model in paper 1 (hereafter referred to as model 1). Figure 4 also shows the error in equilibrium relative humidity that corresponds to a change of ± 0.01 in ϕ (right-hand scale). The edb data are uncertain by at least this amount, equivalent to $\pm 0.25\%$ in relative humidity. The relative humidity in equilibrium with a saturated solution of $(NH_4)_2SO_4$ at 298.15 K is 80.2%.

3.3. $NH_4NO_3-H_2O$. The thermodynamic data for this system are listed in Table 3 of paper 1. The fit of the model is here limited to a maximum of 27.07 mol kg^{-1} and includes only isopiestic measurements. The result is shown in Figure 5, where it is compared with both model 1 and the earlier critical evaluation of Hamer and Wu.[22] The deviations between model 1 and the present fit correspond to maximum differences of about 0.2% in equilibrium relative humidity. The equilibrium relative humidity above a saturated solution of NH_4NO_3 at 298.15 K is 61.2%.

3.4. NH_4Cl-H_2O. Sources of activity data for this system are listed in Table 5 and consist of freezing point data (which were converted to osmotic coefficients at 298.15 K) and isopiestic and edb measurements. The data were fitted to a maximum molality of 7.5 mol kg^{-1} (approximately the saturation molality), with the edb determinations excluded and with

TABLE 5: Sources of Activity Data at 298.15 K for NH_4Cl-H_2O Solutions

m^a				
min	max	used[b]	data type[c]	source
2.026	7.390	yes	iso	Wishaw and Stokes[60]
1.904	7.418	yes	iso	Shul'ts et al.[63]
2.467	6.892	yes	iso	Kirgintsev and Lukyanov[62]
0.00373	0.1022	yes	fp[d]	Garnsey and Prue[61]
6.036	21.78	no[e]	edb	Liang and Chan[92]

[a] Molality. [b] Used in the fit of the model. [c] Type of measurement: iso, isopiestic measurements; fp, freezing point depression; edb, electrodynamic balance measurements of the water activity/concentration relationship for supersaturated solutions. [d] Converted to osmotic coefficients at 298.15 K using available thermal data. [e] Not used, as the fit was restricted to subsaturated solutions only.

parameter $V_{1,NH4\cdot Cl}$ fixed to -1.25. The result is shown in Figure 6, where it is also compared with the previous critical assessment of Hamer and Wu.[22] The scatter of the isopiestic data, about ± 0.002 in ϕ, corresponds to an uncertainty of only $\pm 0.04\%$ in relative humidity. The equilibrium relative humidity above a saturated solution of NH_4Cl at 298.15 K is 77.2%.

3.5. $Na_2SO_4-H_2O$, $NaNO_3-H_2O$, and $NaCl-H_2O$. Aqueous solutions of these salts and their mixtures have been modeled to high supersaturation by Chan et al.[24] and by Clegg et al.[17] Sources of activity data for aqueous Na_2SO_4 are summarized in Table 3 of Clegg et al.[17] In the model of Clegg et al.[17] the osmotic and activity coefficients of aqueous Na_2SO_4 are represented to about 14 mol kg^{-1} (compared to a saturation with respect to $Na_2SO_4 \cdot 10H_2O_{(cr)}$ at only 1.97 mol kg^{-1}), although accepting quite large deviations of the fitted model from the experimental data. In particular, a rising trend in water activity is predicted for molalities above about 12 mol kg^{-1}, which is not realistic (see Figure 3 of Clegg et al.[17]). In this work we use data from sources listed by Clegg et al.,[17] but restrict the maximum molality of fit to 6 mol kg^{-1}. The result is plotted in Figure 7. The model represents the data to within experimental precision over the concentration range fitted, with a worthwhile improvement in accuracy over the extended fit of Clegg et al.[17] The equilibrium relative humidity of a saturated solution of Na_2SO_4 at 298.15 K is 93.6%.

The work of Clegg et al.[17] shows that the relative humidity/concentration relationship for aqueous $NaNO_3$ at 298.15 K can be represented by the model to molalities exceeding 100 mol kg^{-1} (for which the water activity is 0.2), to about the same precision as the measurements. Sources of thermodynamic data are listed in Table 2 of Clegg et al.[17] Here we have taken the opportunity to restandardize the osmotic coefficients of Robinson[25] and Bezboruah et al.[26] to new values for the aqueous KCl isopiestic standard (D. G. Archer, personal communication, 1997) and have refitted to the same maximum molality of 132.9 mol kg^{-1}. The result is shown in Figure 8 and is compared with the evaluation of Hamer and Wu[22] for subsaturated solutions. The uncertainty in the edb measurements of ± 0.01 to ± 0.02 in ϕ corresponds to a maximum change of about $\pm 0.25\%$ in equilibrium relative humidity. The relative humidity above a saturated solution of $NaNO_3$ at 298.15 K is 73.9%.

Sources of activity data at 298.15 K for aqueous NaCl are listed in Table 1 of Clegg et al.[17] Here, osmotic coefficients from the critical evaluation of Archer[27] and the edb studies of Tang et al.,[28] Cohen,[29] and Chan et al.[24] have been fitted to a molality of 8 mol kg^{-1}. The result is shown in Figure 9, where it is also compared with the results of Clegg et al.[17] (for compositions including some supersaturated solutions) and the evaluation of Hamer and Wu (1972). The improvement in accuracy for subsaturated solutions, compared to the work of Clegg et al.,[17] is up to about 0.6% in equilibrium relative humidity. The relative humidity above a saturated solution of NaCl at 298.15 K is 75.3%.

3.6. $H_2SO_4-HNO_3-H_2O$, $H_2SO_4-HCl-H_2O$, and $HNO_3-HCl-H_2O$. These mixed acid systems have been modeled by Carslaw et al.,[14] who list sources of activity data in their Tables 11 and 13. A large number of thermodynamic measurements, including freezing points and equilibrium $pHNO_3$ and pH_2O measurements, are available for $H_2SO_4-HNO_3-H_2O$ solutions. Carslaw et al.[14] have determined parameters $W_{HSO4\cdot NO3\cdot H}$, $W_{SO4\cdot NO3\cdot H}$, and $U_{HSO4\cdot NO3\cdot H}$ as functions of temperature from these data. In the absence of measurements at 298.15 K, their values (at this temperature) are adopted for the present study and are listed in Table 2.

Solubilities of $HCl_{(g)}$ in aqueous H_2SO_4 have been determined from 248.15 to 343 K.[30,31] Satisfactory agreement with the model was obtained with all ternary interaction parameters set to zero for the mixed solution (see Figure 12 of Carslaw et al.[14]), and these null values are retained here.

There appear to be no satisfactory activity data for $HNO_3-HCl-H_2O$ solutions for the compositions and temperatures of interest to atmospheric chemists, and because of this, it is necessary to set the ternary interaction parameters to zero. However, comparisons of model predictions with partial pressures over $H_2SO_4-HNO_3-HCl-H_2O$ solutions at low temperature measured by Elrod et al.[32] show excellent agreement, which gives confidence in these parameter values.

3.7. $H_2SO_4-(NH_4)_2SO_4-H_2O$, $HNO_3-NH_4NO_3-H_2O$, $(NH_4)_2SO_4-NH_4NO_3-H_2O$, and $NH_4HSO_4-NH_4NO_3-H_2O$. Sources of activities for these systems are listed in Tables 4−7 of paper 1. The data have been refitted for the present model using the pure (single-solute) parameters listed in Table 1. For the $H_2SO_4-(NH_4)_2SO_4-H_2O$ system it was possible to retain a fit extending into the supersaturated region; for example the edb data of Spann[33] for aqueous NH_4HSO_4 are fitted to just over 90.78 mol kg^{-1} (a relative humidity of 19.4%) and acid ammonium salt solubilities to about 27 mol kg^{-1} H_2SO_4, as is shown in Figure 20 of paper 1. Due to the optimization of $NH_4^+-SO_4^{2-}$ interaction parameters for subsaturated solutions, it is likely that the present model is more accurate for such concentrations, at least for mixtures in which $(NH_4)_2SO_4$ is the major component. For solutions containing chiefly H_2SO_4 the liquid phase extends essentially to the pure acid, which is beyond the limit of either model (40 mol kg^{-1}, an H_2SO_4 mole fraction of 0.419). Nonetheless, both the present model and that in paper 1 represent the solubility curve to relative humidities of <10%. Calculated relative humidities above solutions simultaneously saturated with respect to $(NH_4)_2SO_{4(cr)}$ and $(NH_4)_3H(SO_4)_{2(cr)}$ are 68.6% (model 1) and 68.8% (the present model), and for solutions saturated with respect to $(NH_4)_3H(SO_4)_{2(cr)}$ and $NH_4HSO_{4(cr)}$ they are 36.7% (model 1) and 36.8% (the present model).

For $HNO_3-NH_4NO_3-H_2O$ mixtures the solubilities of NH_4NO_3 (Table 5) have been fitted to a maximum molality of 20 mol kg^{-1} HNO_3 here, compared to 25 mol kg^{-1} for model 1. This slightly reduced concentration is consistent with the lower maximum molality of fit for aqueous HNO_3 used in the present model. The data for the pK_a^* of NH_4^+ in aqueous NH_4NO_3 are represented to about the same level of accuracy for both models (see Figure 9 of paper 1 for the model 1 result). The calculated relative humidity, above a 10 mol kg^{-1} HNO_3 solution saturated with NH_4NO_3 is 45.7% (model 1) and 45.8% (the present model), indicating good consistency. The difference

TABLE 6: Sources of Activity Data at 298.15 K for $H_2SO_4-Na_2SO_4-H_2O$ Solutions

m^a min	m^a max	used[b]	data type[c]	source
1.974	>100	yes	sol	Silcock[55]
0.734	17.08	yes	sol	Foote[80]
0.158	17.72	yes	ϕ	Rard[75,76]
0.0202	0.109	yes	emf	Covington et al.[79]
0.0300	1.10	yes	emf	Harned and Sturgis[78]
0.200	2.00	yes	emf	Randall and Langford[77]
7.401	>100	yes	edb	Tang and Munkelwitz[70]

[a] Total molality ($mH_2SO_4 + mNa_2SO_4$). [b] Used in the fit of the model. [c] Type of measurement: sol, salt solubility; ϕ, osmotic coefficient from isopiestic experiments; emf, electromotive force determination of H_2SO_4 activity; edb, electrodynamic balance measurements of the water activity/concentration relationship for supersaturated solutions.

rises to ~2% at 20 mol kg^{-1} HNO_3, the limit of the present fit. It is likely that model 1 is more accurate at this and higher concentrations, because of the larger array of ternary data used in the parameterization and also the extended range of fit of the two binary components.

In the parameterization of the model for $(NH_4)_2SO_4-NH_4NO_3-H_2O$ mixtures (see Table 7 of paper 1 for sources of data), the water partial pressure measurements of Emons and Hahn[34] at 298.15 K were included in the data set, and the edb measurements of Chan et al.[35] for supersaturated solutions were omitted. As a comparison between the models, the calculated relative humidities above solutions simultaneously saturated with respect to $(NH_4)_2SO_{4(cr)}$ and $(NH_4)_2SO_4 \cdot 2NH_4NO_{3(cr)}$ are 63.5% (model 1) and 66.2% (the present model), for $(NH_4)_2SO_4 \cdot 2NH_4NO_{3(cr)}$ and $(NH_4)_2SO_4 \cdot 3NH_4NO_{3(cr)}$ they are 64.5% (model 1) and 63.5% (the present model), and for $(NH_4)_2SO_4 \cdot 3NH_4NO_{3(cr)}$ and $NH_4NO_{3(cr)}$ they are 60.4% (model 1) and 60.1% (the present model). The differences for the first two transitions mostly reflect variations in the predicted concentrations of the saturated solutions, which are within the uncertainty of the data (Figure 22 of paper 1). However, there remain differences of about 0.4% in relative humidity between the model predictions when the same solution compositions are used, due to variations in the calculated activities.

For the $NH_4HSO_4-NH_4NO_3-H_2O$ system, for which there are measurements of the solubility of $NH_4HSO_4 \cdot NH_4NO_{3(cr)}$, $NH_4HSO_{4(cr)}$, and $NH_4NO_{3(cr)}$ (Table 8 of paper 1), the same data were fitted for both model 1 and the present model, although here only results for 298.15 K were used. At this temperature the equilibrium constants ${}^xK_S(NH_4HSO_4 \cdot NH_4NO_3)$ for the two models differ by about 45%. Model 1 is likely to be more accurate for calculating the properties of this system because of the very high aqueous-phase concentrations at which solid phases precipitate. Calculated relative humidities above a solution saturated with respect to both $NH_4HSO_{4(cr)}$ and $NH_4HSO_4 \cdot NH_4NO_{3(cr)}$ are very similar (29.8% for model 1, and 29.3% for the present model), although the compositions of the saturated solutions differ (46.6 mol kg^{-1} NH_4HSO_4 and 14.66 mol kg^{-1} NH_4NO_3 for model 1; 41.1 mol kg^{-1} NH_4HSO_4 and 15.8 mol kg^{-1} NH_4NO_3 for the present model).

3.8. $H_2SO_4-Na_2SO_4-H_2O$. Sources of data available for this system are listed in Table 6 and comprise extensive measurements of osmotic coefficients, and emf studies which yield the H_2SO_4 activity, salt solubilities, and edb measurements of water activity. The solubility curve of this mixture is complex, with the following series of solids precipitated at 298.15 K as aqueous H_2SO_4 concentration is increased: $Na_2SO_4 \cdot 10H_2O_{(cr)}$, $Na_2SO_{4(cr)}$, $Na_3H(SO_4)_{2(cr)}$, $NaHSO_4 \cdot H_2O_{(cr)}$, and $NaHSO_{4(cr)}$ within the fitted range of the model. In solutions containing over 21 mol kg^{-1} $H_2SO_{4(aq)}$ hydrated and anhydrous forms of $NaH_3(SO_4)_2$ occur. The solid $Na_3H(SO_4)_2 \cdot H_2O_{(cr)}$ has been claimed to occur from about 3 to 5.5 mol kg^{-1} $H_2SO_{4(aq)}$,[36] but appears to be metastable at best. Following Harvie et al.,[37] we have excluded it from the model.

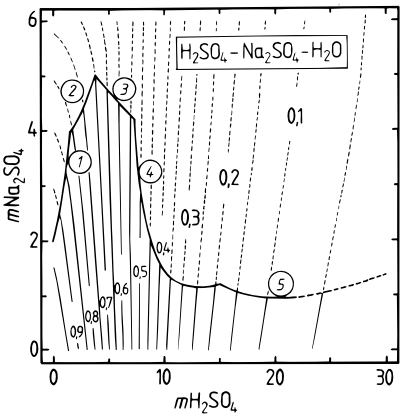

Figure 10. Phase diagram of $H_2SO_4-Na_2SO_4-H_2O$ at 298.15 K and equilibrium water activities for both subsaturated and supersaturated solutions. Compositions are given as molalities. Lines: solid (heavy), solubilities of the following solid phases: (1) $Na_2SO_4 \cdot 10H_2O_{(cr)}$; (2) $Na_2SO_{4(cr)}$; (3) $Na_3H(SO_4)_{2(cr)}$; (4) $NaHSO_4 \cdot H_2O_{(cr)}$; (5) $NaHSO_{4(cr)}$. Contours: equilibrium water activities, with values as marked. Contours are dotted for supersaturated solutions.

The $H_2SO_4-Na_2SO_4-H_2O$ mixture contains four ions; consequently there are four possible sets of triplet interaction parameter within the model in addition to the unknown binary $Na^+-HSO_4^-$ terms. Figure 24 shows salt solubilities at 298.15 K, together with the range of compositions for which osmotic coefficients have been determined. The coverage is extensive, except for solutions containing mostly H_2SO_4, and the large number of measurements is sufficient to constrain the model well.

Electromotive force data were converted from international volts to volts, and standard emfs ($E°$) were determined as described by Harvie et al.[37] The osmotic coefficients and emf measurements were fitted by the model to a maximum total molality of 15 mol kg^{-1} and salt solubilities to 23 mol kg^{-1} in order to determine the equilibrium constant for $NaHSO_4$ formation. The result of the fit is shown in Figures 25−27 and shows excellent agreement with the measured solubilities and emfs (here shown as $f_{H_2SO_4}$*) and only small deviations in the cases of the osmotic coefficients (Figure 26). Using data tabulated in the Gmelin handbook,[38] we have also determined a tentative value of ${}^xK_S(NaH_3(SO_4)_2 \cdot H_2O)$; see Table 3.

The calculated solubility curve and contours of water activity are shown in Figure 10 and exhibit markedly different behavior from electrolyte systems in which there is little or no ion association. Here, for H_2SO_4 molalities between about 7 and 10 mol kg^{-1}, water activity is almost invariant with Na_2SO_4 concentration (to 6 mol kg^{-1} of salt, the limit shown in the figure). Furthermore, for acid molalities above about 10 mol kg^{-1} the addition of Na_2SO_4 *increases* the equilibrium relative humidity above the solution. This behavior is qualitatively similar to that of $H_2SO_4-(NH_4)_2SO_4-H_2O$ and confirms the importance of the explicit recognition of the $HSO_4^-{}_{(aq)} \rightleftharpoons H^+{}_{(aq)} + SO_4^{2-}{}_{(aq)}$ equilibrium within the model in order to represent the observed behavior of the system.

3.9. $HNO_3-NaNO_3-H_2O$. The only sources of activity data for this system (Table 7) are salt solubilities—though over a wide range of temperature—and a very few partial pressure

TABLE 7: Sources of Activity Data at 298.15 K for $HNO_3-NaNO_3-H_2O$ Solutions

m^a				
min	max	used[b]	data type[c]	source
10.38	85.66	yes	sol[d]	Gmelin Handbook[38]
9.476	85.82	yes	sol	Kurnakov and Nikolaev[82]
17.09	24.99	yes	$pHNO_3$, pH_2O[e]	Flatt and Benguerel[81]
6.00	6.00	no[f]	$pHNO_3$	Clegg and Brimblecombe[93]

[a] Total molality ($mHNO_3 + mNaNO_3$). [b] Used in the fit of the model. [c] Type of measurement: sol, solubility of $NaNO_3$; $pHNO_3$, equilibrium partial pressure of HNO_3; pH_2O, equilibrium partial pressure of H_2O. [d] Values in the Gmelin Handbook are based upon Kurnakov and Nikolaev[82] and other work by the same authors. [e] Data were converted to mean activity coefficients of HNO_3 and to water activity. [f] Only a single partial pressure was measured.

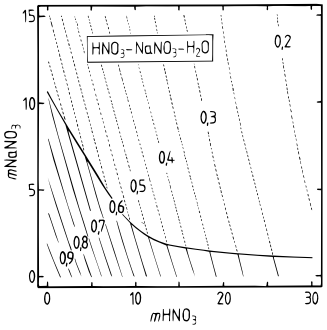

Figure 11. Phase diagram of $HNO_3-NaNO_3-H_2O$ at 298.15 K and equilibrium water activities for both subsaturated and supersaturated solutions. Compositions are given as molalities. Lines: solid (heavy), solubility of $NaNO_3$ in $HNO_{3(aq)}$; contours, equilibrium water activities with values as marked. Contours are dotted for supersaturated solutions.

TABLE 8: Sources of Activity Data at 298.15 K for $HCl-NH_4Cl-H_2O$ Solutions

m^a				
min	max	used[b]	data type[c]	source
0	19.29[d]	yes	sol	Silcock[55]
0.25	3.00	yes	emf[e]	Robinson et al.[39]
1.00	1.00	yes	emf[e]	Chan et al.[40]
0.10	3.00	yes	emf[e]	Downes et al.[41]
0.512	6.480	yes	pK_a*[f]	Maeda et al.[42]
10.39	16.73	yes[g]	pHCl	Silcock[55]
5.00	5.00	no[h]	pHCl	Clegg and Brimblecombe[94]

[a] Total molality (mHCl + $m$$NH_4Cl$). [b] Used in the fit of the model. [c] Type of measurement: sol, solubility of NH_4Cl, emf, electromotive force measurement of HCl activity, pK_a*, acid dissociation constant of NH_4^+ in aqueous NH_4Cl. [d] Molality range of aqueous HCl. [e] Converted to mean activity coefficients of HCl. [f] Converted to the reciprocal of NH_4^+ and H^+ activity coefficients using γ_{NH_3} from the work of Maeda et al.[42] [g] Only a single measurement was used (out of a total of four). [h] Only one composition was measured.

measurements for solutions containing low molalities of $NaNO_3$. Interaction parameters $W_{H\cdot Na\cdot NO3}$ and $U_{H\cdot Na\cdot NO3}$ were determined from the data, and the results are shown in Figures 28 and 29. The calculated solubility curve and equilibrium water activities are shown in Figure 11.

3.10. $HCl-NH_4Cl-H_2O$. Sources of activity data for this system are listed in Table 8 and comprise $NH_4Cl_{(cr)}$ solubilities, emf determinations of HCl activities, the pK_a* of $NH_4^+{}_{(aq)}$ (from potentiometric titration), and a very few partial pressure measurements. Activity coefficients of HCl were calculated from the emf measurements of Robinson et al.[39] using their listed standard emfs ($E°$) and taken directly from the tabulations of Chan et al.[40] and Downes et al.[41]

At 298.15 K the properties of this system are comparatively well studied. The fits of the model to the emf measurements and salt solubilities (see Figures 30 and 31) agree well with the data over the full range of compositions and concentrations. The pK_a* determinations of Maeda et al.[42] were not included in the fit, but are compared with predictions in Figure 32 as a test. For this purpose they were first converted from $[K_a\gamma_{NH_4}/(\gamma_H\gamma_{NH_3})]$ to $f_{NH_4}*/f_H*$ using the known thermodynamic dissociation constant[43] and activity coefficients of NH_3 derived by Maeda et al.[42] Agreement with the model is satisfactory, although the reason for the small positive offset of the data and the fact that they do not appear to extrapolate monotonically to unity at zero ionic strength is not known.

Figure 12 shows the calculated solubility curve with contours of equilibrium relative humidity superimposed.

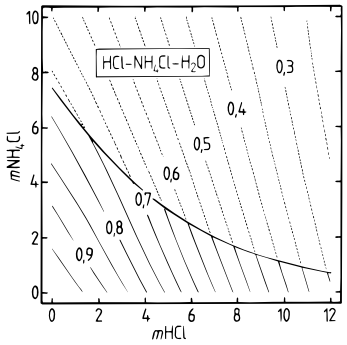

Figure 12. Phase diagram of $HCl-NH_4Cl-H_2O$ at 298.15 K and equilibrium water activities for both subsaturated and supersaturated solutions. Compositions are given as molalities. Lines: solid (heavy), solubility of $NH_4Cl_{(cr)}$ in $HCl_{(aq)}$; contours, equilibrium water activities, with values as marked. Contours are dotted for supersaturated solutions.

TABLE 9: Sources of Activity Data at 298.15 K for $HCl-NaCl-H_2O$ Solutions

m^a				
min	max	used[b]	data type[c]	source
6.054	19.024	yes	sol	Silcock[55]
3.00	6.00	yes	emf	Hawkins[83]
1.00	3.00	yes	emf	Harned[84]
0.100	0.8720	yes	emf	Macaskill et al.[44]
1.00	1.00	yes	emf	Chan et al.[40]
5.00	5.00	no[d]	pHCl	Clegg and Brimblecombe[94]

[a] Total molality (mHCl + mNaCl). [b] Used in the fit of the model. [c] Type of measurement: sol, solubility of NaCl; emf, electromotive force measurement (yields γ_{HCl}); pHCl, equilibrium partial pressure of HCl. [d] Only a single partial pressure was measured.

3.11. $HCl-NaCl-H_2O$. Data for this system, Table 9, consist chiefly of emf measurements of HCl activity (which extend over a wide range of temperatures) and NaCl solubilities in aqueous HCl. The emfs of Macaskill et al.[44] were converted to f_{HCl}* as described by Clegg and Whitfield,[20] and values of the mean activity coefficient given in the other studies were used directly. Measured and fitted activity coefficients from all sources are compared in Figure 33 and agree well over the full range of ionic strength to 6 mol kg^{-1}. The observed solubilities are also represented well, Figure 34. The calculated solubility curve, with contours of water activity superimposed, is shown in Figure 13.

3.12. $(NH_4)_2SO_4-NH_4Cl-H_2O$. Data for this system consist of solubilities of $(NH_4)_2SO_{4(cr)}$ and $NH_4Cl_{(cr)}$, and sources are listed in Table 10. The measurements were used to determine values of $Q_{1,SO4\cdot Cl\cdot NH4}$ and $U_{SO4\cdot Cl\cdot NH4}$, and the result of the fit is shown in Figure 35. Calculated solubilities, together with contours of water activity, are shown in Figure 14.

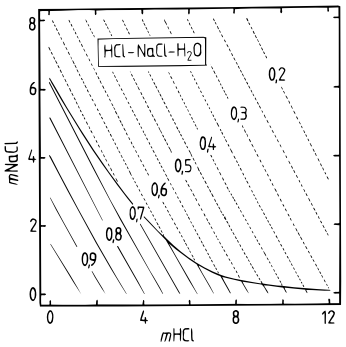

Figure 13. Phase diagram of $HCl-NaCl-H_2O$ at 298.15 K and equilibrium water activities for both subsaturated and supersaturated solutions. Compositions are given as molalities. Lines: solid (heavy), solubility of NaCl in $HCl_{(aq)}$; contours, equilibrium water activities, with values as marked. Contours are dotted for supersaturated solutions.

TABLE 10: Sources of Activity Data at 298.15 K for $(NH_4)_2SO_4-NH_4Cl-H_2O$ Solutions

m^a				
min	max	used[b]	data type[c]	source
5.756	8.796	yes	sol	Silcock[55]
8.749	8.749[d]	yes	sol	Hill and Loucks[85]

[a] Total molality ($m(NH_4)_2SO_4 + mNH_4Cl$). [b] Used in the fit of the model. [c] Type of measurement: sol, salt solubility. [d] A single measurement of simultaneous saturation with respect to both solid phases.

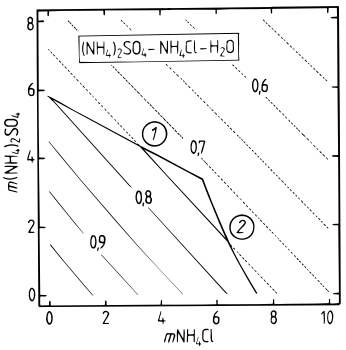

Figure 14. Phase diagram of $(NH_4)_2SO_4-NH_4Cl-H_2O$ at 298.15 K and equilibrium water activities for both subsaturated and supersaturated solutions. Compositions are given as molalities. Lines: solid (heavy), solubilities of the following solid phases: (1) $(NH_4)_2SO_{4(cr)}$; (2) $NH_4Cl_{(cr)}$. Contours: equilibrium water activities, with values as marked. Contours are dotted for supersaturated solutions.

TABLE 11: Sources of Activity Data at 298.15 K for $NH_4NO_3-NH_4Cl-H_2O$ Solutions

m^a				
min	max	used[b]	data type[c]	source
7.390	30.70	yes	sol	Silcock[55]
6.107	55.46	no	edb	Liang and Chan (unpublished)

[a] Total molality ($mNH_4NO_3 + mNH_4Cl$). [b] Used in the fit of the model. [c] Type of measurement: sol, salt solubility; edb, electrodynamic balance measurements of the water activity/concentration relationship for supersaturated solutions.

3.13. $NH_4NO_3-NH_4Cl-H_2O$. The available data for this system, Table 11, comprise solubilities of $NH_4NO_{3(cr)}$ and $NH_4Cl_{(cr)}$ and unpublished edb measurements of water activities for very concentrated solutions (which are not used in this model). Measured and fitted salt solubilities are shown in Figure 36, with calculated contours of water activity superimposed. Note that, when the model parameters were determined, the activity product of $NH_4NO_{3(cr)}$ was adjusted to the measured solubility for pure aqueous NH_4NO_3 shown in Figure 36 in order to avoid bias in the result. This solubility (26.22 mol kg^{-1}) is slightly lower than found in other studies (see Figure 40 and also paper 1) and greater than the value used to determine the equilibrium constant in Table 3 (26.79 mol kg^{-1}). The calculated solubility curve and equilibrium water activities are shown in Figure 15.

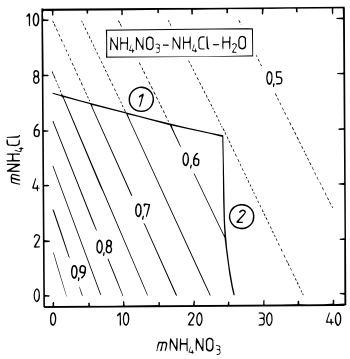

Figure 15. Phase diagram of $NH_4NO_3-NH_4Cl-H_2O$ at 298.15 K and equilibrium water activities for both subsaturated and supersaturated solutions. Compositions are given as molalities. Lines: solid (heavy), solubilities of the following solid phases: (1) $NH_4Cl_{(cr)}$; (2) $NH_4NO_{3(cr)}$. Contours: equilibrium water activities, with values as marked (and dotted for supersaturated solutions).

TABLE 12: Sources of Activity Data at 298.15 K for $(NH_4)_2SO_4-Na_2SO_4-H_2O$ Solutions

m^a				
min	max	used[b]	data type[c]	source
1.952	6.562	yes	sol	Silcock[55]
4.551	6.400	yes	sol	Sborgi et al.[87]
1.96	6.450	yes	sol	Filippov et al.[86]
1.685	5.747	yes	ϕ	Filippov et al.[86]
1.590	5.088	no	ϕ	Kotlyar-Shapirov and Kirgintsev[95]
~2	~26	no	edb[d]	Tang[96]

[a] Total molality ($m(NH_4)_2SO_4 + mNa_2SO_4$). [b] Used in the fit of the model. [c] Type of measurement: sol, salt solubility; ϕ, isopiestic measurement of water activity; edb, electrodynamic balance measurements of the water activity/concentration relationship for supersaturated solutions. [d] Presented as fitted equations.

3.14. $(NH_4)_2SO_4-Na_2SO_4-H_2O$. Table 12 lists sources of activity data for this system, which include osmotic coefficients, solubilities of $(NH_4)_2SO_{4(cr)}$, $Na_2SO_{4(cr)}$, and the double salt $(NH_4)_2SO_4 \cdot Na_2SO_4 \cdot 4H_2O_{(cr)}$, and edb measurements for supersaturated solutions (not used for the present model). The results of the fit are shown in Figures 37 and 38, with good agreement between the model and both types of data. An activity product (^xK_S) of 6.914×10^{-13} for the double salt was determined in the fit. The calculated solubility curve, with water activities superimposed, is shown in Figure 16.

3.15. $NH_4NO_3-NaNO_3-H_2O$. Osmotic coefficients and $NH_4NO_{3(cr)}$ and $NaNO_{3(cr)}$ solubilities have been determined for this system; see Table 13. Bergman and Shulyak[45] and Timoshenko[46] have found a double salt, $NH_4NO_3 \cdot 2NaNO_{3(cr)}$, which occurs in solutions concentrated with respect to both NH_4NO_3 and $NaNO_3$. However, this phase was not noted in either of the vapor pressure studies listed in Table 13, nor does it appear to have been found at other temperatures except by Bergman and Shulyak.[45] In the principal fit of the model, on the basis of the osmotic coefficients of Kirgintsev and Lukyanov[47] and salt solubilities, we have assumed that the double-salt compositions are in fact $NaNO_{3(cr)}$ (see Figures 39 and 40). However, the possibility remains that the double salt is a metastable or even stable solid phase, and the fit has therefore been repeated and the activity product of $NH_4NO_3 \cdot 2NaNO_{3(cr)}$

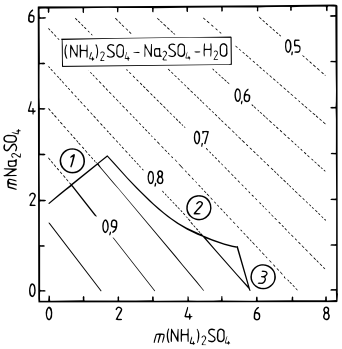

Figure 16. Phase diagram of $(NH_4)_2SO_4-Na_2SO_4-H_2O$ at 298.15 K and equilibrium water activities for both subsaturated and supersaturated solutions. Compositions are given as molalities. Lines: solid (heavy), solubilities of the following solid phases: (1) $Na_2SO_4 \cdot 10H_2O_{(cr)}$; (2) $Na_2SO_4 \cdot (NH_4)_2SO_4 \cdot 4H_2O_{(cr)}$; (3) $(NH_4)_2SO_{4(cr)}$. Contours: equilibrium water activities, with values as marked. Contours are dotted for supersaturated solutions.

TABLE 13: Sources of Activity Data at 298.15 K for $NH_4NO_3-NaNO_3-H_2O$ Solutions

m^a				
min	max	used[b]	data type[c]	source
10.56	34.63	yes	sol	Silcock[55]
10.56	32.39	yes[d]	sol	Bergman and Shulyak[45]
34.07	34.07	no[e]	sol	Shpunt[97]
32.45	32.46	yes[f]	sol	Timoshenko[46]
4.186	12.64	yes	ϕ	Kirgintsev and Lukyanov[47]
7.049	35.8	no	edb	Liang and Chan (unpublished)
sat.[g]		no	pH_2O	Dingemans and Dijkgraaf[48]
sat.[g]		no	pH_2O	Prideaux[49]

[a] Total molality ($mNH_4NO_3 + mNaNO_3$). [b] Used in the fit of the model. [c] Type of measurement: sol, salt solubility; ϕ, isopiestic measurement of water activity; edb, electrodynamic balance measurements of the water activity/concentration relationship for supersaturated solutions; pH_2O, equilibrium water partial pressure. [d] The double salt that has been found by some workers (including Bergman and Shulyak) was assumed to be $NaNO_{3(cr)}$ in the principal fit of the model. [e] Only a single measurement at 298.15 K. [f] Only two compositions listed, double-salt found. [g] An aqueous solution simultaneously saturated with respect to $NaNO_{3(cr)}$ and $NH_4NO_{3(cr)}$.

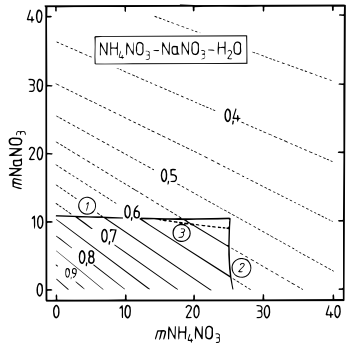

Figure 17. Phase diagram of $NH_4NO_3-NaNO_3-H_2O$ at 298.15 K and equilibrium water activities for both subsaturated and supersaturated solutions. Compositions are given as molalities. Lines: solid (heavy), solubilities of the following solid phases: (1) $NaNO_{3(cr)}$, (2) $NH_4NO_{3(cr)}$; dotted (heavy), (3) $2NaNO_3 \cdot NH_4NO_{3(cr)}$. Contours: equilibrium water activities, with values as marked. Contours are dotted for supersaturated solutions.

determined. The solubility curve for $NH_4NO_3 \cdot 2NaNO_{3(cr)}$ is also shown in Figure 40, and there is, for this case, improved agreement between the measurements and fitted solubilities and also the osmotic coefficients (not shown). However, the equilibrium partial pressures of water over solutions stated as being saturated with respect to both $NH_4NO_{3(cr)}$ and $NaNO_{3(cr)}$ (Table 13) are more consistent with these two salts being the equilibrium solid phases. The model yields $a_1 = 0.5085$ (equivalent to a partial pressure of 12.08 mmHg) for a solution saturated with respect to $NH_4NO_{3(cr)}$ and $NaNO_{3(cr)}$, compared with measured values of 11.7 mmHg[48] and 11.6 mmHg.[49] For solutions saturated with respect to $NH_4NO_{3(cr)}$ and $NH_4NO_3 \cdot 2NaNO_{3(cr)}$ the calculated equilibrium partial pressure of water would be higher, because of the lower total concentration of salts in the aqueous phase.

The model parameters obtained in the principal model fit are listed in Table 2, and those obtained for the case of double-salt formation given in the notes to Table 3. Figure 17 shows the calculated solubility curves for the system, with water activities superimposed. Here the scale for $NaNO_{3(aq)}$ is extended, as the

TABLE 14: Sources of Activity Data at 298.15 K for $NH_4Cl-NaCl-H_2O$ Solutions

m^a				
min	max	used[b]	data type[c]	source
6.150	8.857	yes	sol	Silcock[55]
8.789	8.789[d]	yes	sol	Sborgi and Franco[90]
2.287	6.602	yes	ϕ	Kirgintsev and Lukyanov[88]
2.167	4.582	yes	ϕ	Maeda et al.[89]

[a] Total molality ($mNH_4Cl + mNaCl$). [b] Used in the fit of the model. [c] Type of measurement: sol, salt solubility; ϕ, isopiestic measurement of water activity. [d] A single measurement of simultaneous saturation with respect to both solid phases.

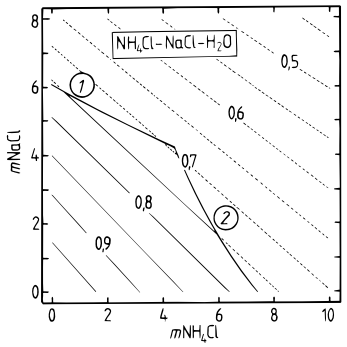

Figure 18. Phase diagram of $NH_4Cl-NaCl-H_2O$ at 298.15 K and equilibrium water activities for both subsaturated and supersaturated solutions. Compositions are given as molalities. Lines: solid (heavy), solubilities of the following solid phases: (1) $NaCl_{(cr)}$; (2) $NH_4Cl_{(cr)}$. Contours: equilibrium water activities, with values as marked. Contours are dotted for supersaturated solutions.

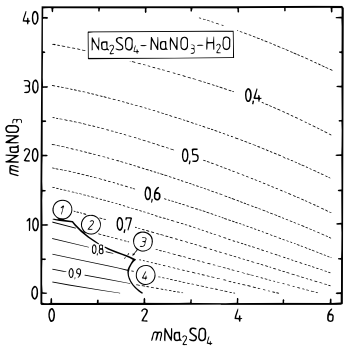

Figure 19. Phase diagram of $Na_2SO_4-NaNO_3-H_2O$ at 298.15 K and equilibrium water activities for both subsaturated and supersaturated solutions. Compositions are given as molalities. Lines: solid (heavy), solubilities of the following solid phases: (1) $NaNO_{3(cr)}$; (2) $NaNO_3 \cdot Na_2SO_4 \cdot H_2O_{(cr)}$; (3) $Na_2SO_{4(cr)}$; (4) $Na_2SO_4 \cdot 10H_2O_{(cr)}$. Contours: equilibrium water activities, with values as marked. Contours are dotted for supersaturated solutions.

TABLE 15: Gibbs Energies of Formation of Acid Sulfate Salts and Other Complex Salts at 298.15 K[a]

salt	$\Delta_f G°$ (kJ mol^{-1})	salt	$\Delta_f G°$ (kJ mol^{-1})
$(NH_4)_3H(SO_4)_2$	−1731.8	$NaHSO_4·H_2O$	−1244.1
NH_4HSO_4	−822.3	$NaHSO_4$	−1003.0
$(NH_4)_2SO_4·2NH_4NO_3$	−1273.3 (−1271.8)	$NaH_3(SO4)_2·H_2O$	−1960.6
$(NH_4)_2SO_4·3NH_4NO_3$	−1458.0 (−1456.1)	$(NH_4)_2SO_4·Na_2SO_4·4H_2O$	−3129.7 (−3121.7)
$NH_4HSO_4·NH_4NO_3$	−1008.0 (−1006.7)	$Na_2SO_4·NaNO_3·H_2O$	−1876.6 (−1874.2)
$Na_3H(SO_4)_2$	−2278.9	$(2NaNO_3·NH_4NO_3)$	−919.5 (−918.4)

[a] The first value listed for each salt was calculated from the equilibrium constant given in Table 3, together with $\Delta_f G°$ for the ions from Wagman et al.[54] and standard thermodynamic relations. The values in parentheses are estimates obtained by adding $\Delta_f G°$ for the individual salts $(NH_4)_2SO_{4(cr)}$, $NH_4NO_{3(cr)}$, and $NH_4HSO_{4(cr)}$ in the appropriate multiples (e.g., $\Delta_f G°(NH_4NO_3·NH_4HSO_{4(cr)}) = \Delta_f G°(NH_4NO_{3(cr)}) + \Delta_f G°(NH_4HSO_{4(cr)})$).

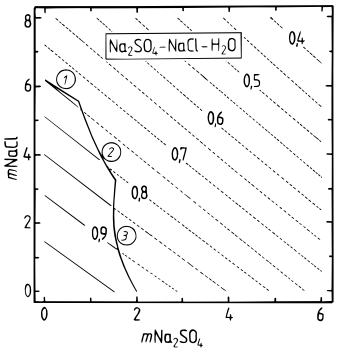

Figure 20. Phase diagram of $Na_2SO_4-NaCl-H_2O$ at 298.15 K and equilibrium water activities for both subsaturated and supersaturated solutions. Compositions are given as molalities. Lines: solid (heavy), solubilities of the following solid phases: (1) $NaCl_{(cr)}$; (2) $Na_2SO_{4(cr)}$; (3) $Na_2SO_4·10H_2O_{(cr)}$. Contours: equilibrium water activities, with values as marked. Contours are dotted for supersaturated solutions.

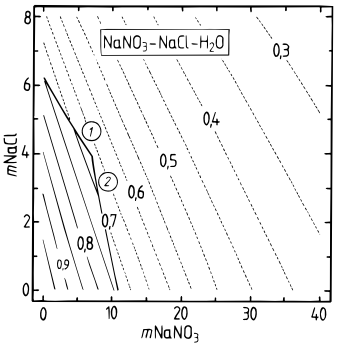

Figure 21. Phase diagram of $NaNO_3-NaCl-H_2O$ at 298.15 K and equilibrium water activities for both subsaturated and supersaturated solutions. Compositions are given as molalities. Lines: solid (heavy), solubilities of the following solid phases: (1) $NaCl_{(cr)}$; (2) $NaNO_{3(cr)}$. Contours: equilibrium water activities, with values as marked. Contours are dotted for supersaturated solutions.

fit of the model to solutions containing this pure component include highly supersaturated solutions.

3.16. $NH_4Cl-NaCl-H_2O$. For this system osmotic coefficients are available from two studies (to water activities as low as 0.787) and measurements of $NH_4Cl_{(cr)}$ and $NaCl_{(cr)}$ solubilities; see Table 14. Measured and fitted quantities are shown in Figures 41 and 42 and agree well for both types of data. The calculated solubility curve, with water activities superimposed, is shown in Figure 18.

3.17. $Na_2SO_4-NaNO_3-H_2O$, $Na_2SO_4-NaCl-H_2O$, and $NaNO_3-NaCl-H_2O$. These systems, including supersaturated solutions, have been studied by Clegg et al.[17] Sources of activity data are listed in their Tables 4−6 and include isopiestic, solubility, and emf and edb measurements. The data have been refitted for the present model, although excluding the edb measurements for supersaturated solutions. This more restricted range of concentrations, and the use of a parameter set for the pure salts that more closely represents the properties of subsaturated $NaCl_{(aq)}$ and $Na_2SO_{4(aq)}$ (see Figures 7 and 9), increase the accuracy of the result by a small amount. For example, the standard deviations of the fits to osmotic coefficients from the studies of Wu et al.[50] and Filippov and Cheremykh[51] for $Na_2SO_4-NaCl-H_2O$ solutions are 0.0032 (present study) and 0.0058 (Clegg et al.[17]). The figure achieved here is close to the precision of the measurements.

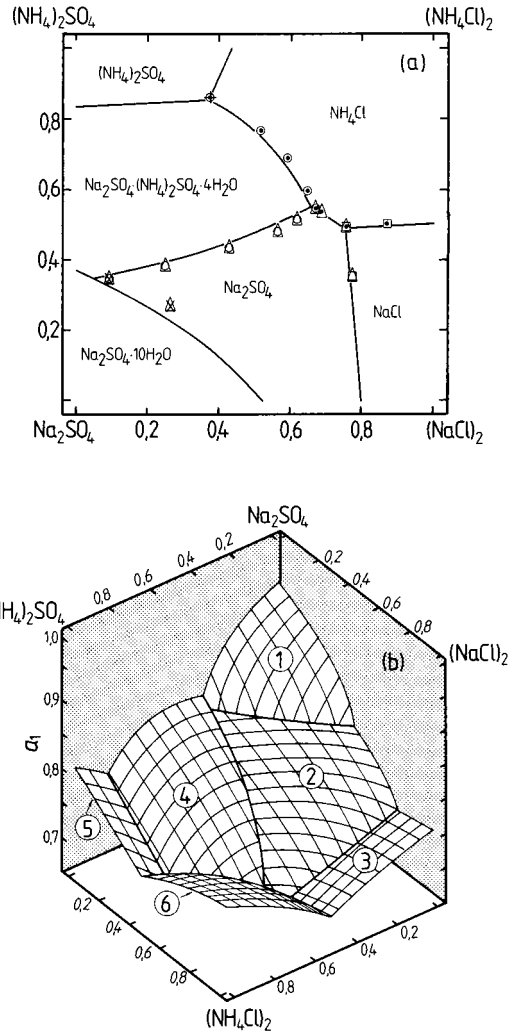

Figure 22. Reciprocal salt diagram for the system $NH_4^+-Na^+-SO_4^{2-}-Cl^--H_2O$ at 298.15 K. (a) Relative compositions of solutions simultaneously saturated with respect to either two or three solid phases. Data are from the compilation of Silcock.[55] Symbols: crosses, $Na_2SO_4·10H_2O_{(cr)}$; open triangles, $Na_2SO_{4(cr)}$; open squares, $NaCl_{(cr)}$; open circles, $Na_2SO_4·(NH_4)_2SO_4·4H_2O_{(cr)}$; pluses, $(NH_4)_2SO_{4(cr)}$; dots, $NH_4Cl_{(cr)}$. Lines: predicted by the model. (b) Calculated water activities (a_1) for the saturated solutions shown in (a). Solid phases: (1) $Na_2SO_4·10H_2O_{(cr)}$; (2) $Na_2SO_{4(cr)}$; (3) $NaCl_{(cr)}$; (4) $Na_2SO_4·(NH_4)_2SO_4·4H_2O_{(cr)}$; (5) $(NH_4)_2SO_{4(cr)}$; (6) $NH_4Cl_{(cr)}$.

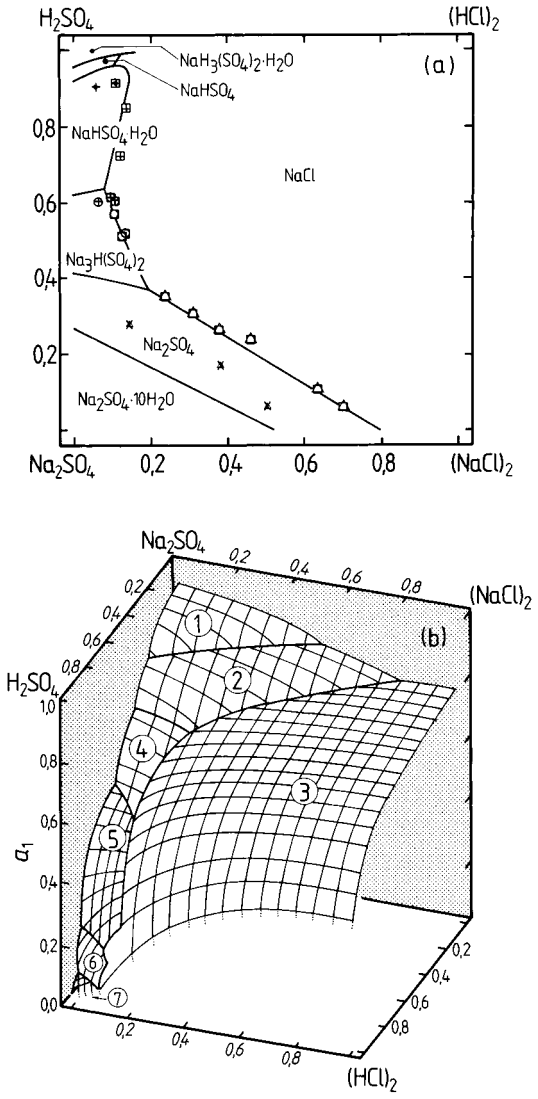

Figure 23. Reciprocal salt diagram for the system $H^+-Na^+-SO_4^{2-}-Cl^--H_2O$ at 298.15 K. (a) Relative compositions of solutions simultaneously saturated with respect to either two or three solid phases. Data are from the compilation of Silcock.[55] Symbols: crosses, $Na_2SO_4{\cdot}10H_2O_{(cr)}$; open triangles, $Na_2SO_{4(cr)}$; open squares, $NaCl_{(cr)}$; open circles, $Na_3H(SO_4)_{2(cr)}$; pluses, $NaHSO_4{\cdot}H_2O_{(cr)}$; dots, $NaHSO_{4(cr)}$. Lines: predicted by the model. (b) Calculated water activities (a_1) for the saturated solutions shown in (a). Solid phases: (1) $Na_2SO_4{\cdot}10H_2O_{(cr)}$; (2) $Na_2SO_{4(cr)}$; (3) $NaCl_{(cr)}$; (4) $Na_3H(SO_4)_{2(cr)}$; (5) $NaHSO_4{\cdot}H_2O_{(cr)}$; (6) $NaHSO_{4(cr)}$; (7) $NaH_3(SO_4)_2{\cdot}H_2O_{(cr)}$.

Calculated solubility curves for all three systems, with contours of water activity, are shown in Figures 19−21.

4. Discussion

The representation of the properties of $(NH_4)_2SO_4-H_2SO_4-H_2O$ mixtures by model 1 is discussed in section 4 of paper 1, including comparisons with measurements of H_2SO_4 partial pressures at 303.15 K[52] and values of $a{NH_4}^+/a{H}^+$ in $(NH_4)_2SO_{4(aq)}$ from dissociation constant measurements at 298.15 K.[53] Much of that material is relevant to the present model. In particular, we note that calculated $a{NH_4}^+/a{H}^+$ activity ratios, required by eq 3 to predict pNH_3, agree with those estimated by model 1 to within 2−4% for aqueous $(NH_4)_2SO_4$ solutions containing 0.0001 mol kg^{-1} H_2SO_4 at 298.15 K.

In this study the equilibrium constants for the formation of 19 solid phases have been determined (see Tables 3 and 15), including several complex salts (containing more than one cation or anion) whose values do not appear to have been determined before. Gibbs energies of formation of the salts are listed in

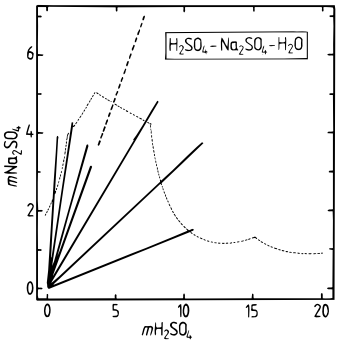

Figure 24. Compositions for which osmotic coefficients of $H_2SO_4-Na_2SO_4-H_2O$ mixtures have been measured at 298.15 K, with the solubility curve (fine dotted line) superimposed. (For the identities of the solid phases, see Figure 27.) Lines: heavy solid, range of data of Rard;[75,76] heavy dotted, range of data of Tang and Munkelwitz[70] (these extend to higher concentrations than shown, beyond the limit of the model).

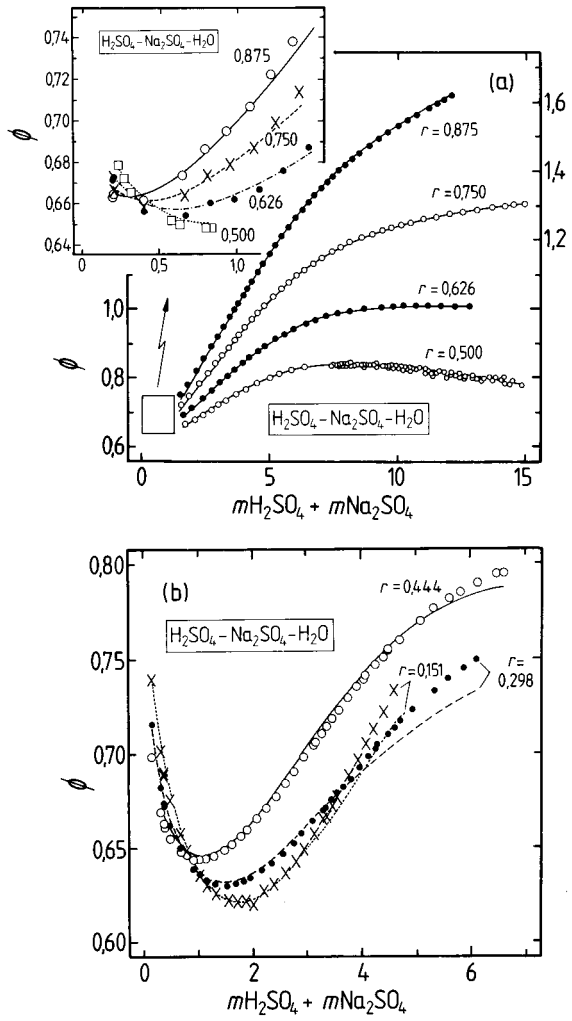

Figure 25. Stoichiometric molal osmotic coefficients (ϕ) of $H_2SO_4-Na_2SO_4-H_2O$ mixtures at 298.15 K, plotted against total molality ($mH_2SO_4 + mNa_2SO_4$). (a) Symbols: data of Rard[75,76] for four different composition ratios r ($mH_2SO_4/(mH_2SO_4 + mNa_2SO_4)$) and of Tang and Munkelwitz[70] for $NaHSO_{4(aq)}$ ($r = 0.5$). Lines: fitted model. The inset shows the data and model fit for total molalities <1.5 mol kg^{-1}. Due to the very large number of measurements carried out by Rard, alternate points only are shown here. (b) Symbols: data of Rard[75,76] for three different composition ratios r. Lines: the fitted model.

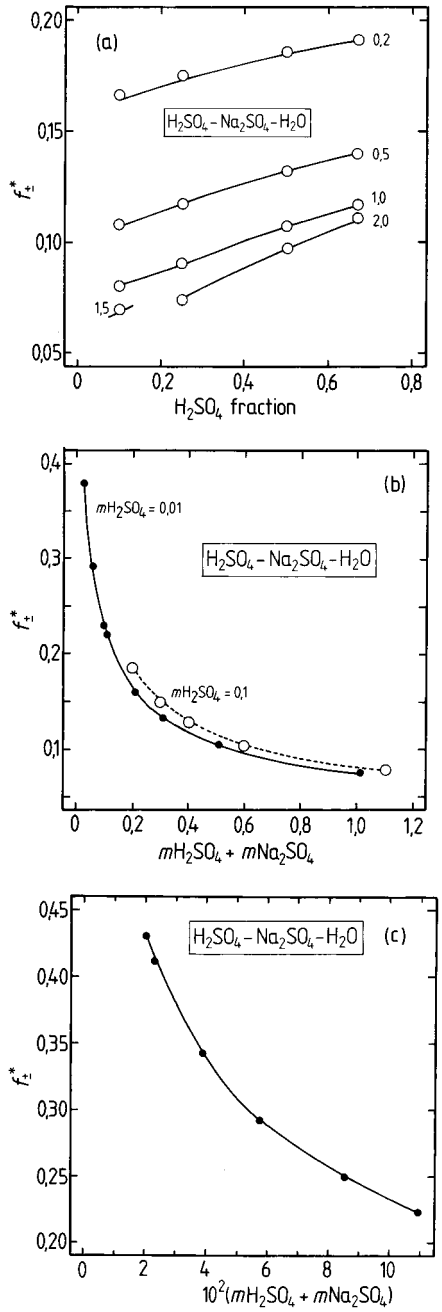

Figure 26. Stoichiometric mean activity coefficients of H_2SO_4 in $H_2SO_4-Na_2SO_4-H_2O$ mixtures at 298.15 K, plotted against H_2SO_4 fraction [$mH_2SO_4/(mH_2SO_4 + mNa_2SO_4)$] and total molality ($mH_2SO_4 + mNa_2SO_4$). (a) Symbols: data of Randall and Langford[77] for five different total molalities (indicated on the plot). (b) Symbols: data of Harned and Sturgis.[78] (c) Symbols: data of Covington et al.[79] In all plots the lines represent the fitted model.

Table 15, together with estimates obtained by a linear combination of $\Delta_fG°$ of the constituent (single) salts. As for model 1, these agree with the fitted values to within a few kJ mol^{-1} although there are much larger absolute differences between the models, up to a maximum of about 90 kJ mol^{-1} for $(NH_4)_2SO_4 \cdot 3NH_4NO_{3(cr)}$. These reflect variations in the ionic activities in the saturated solutions calculated by the two models and also the fact that the solubilities determined by model 1 for 298.15 K are the result of an optimization of the fit over several temperatures. Thus, for example, simultaneous saturation of $NH_4^+-SO_4^{2-}-NO_3^--H_2O$ solutions with respect to $(NH_4)_2SO_{4(cr)}$ and $(NH_4)_2SO_4 \cdot 2NH_4NO_{3(cr)}$ is predicted to occur for compositions [2.85 mol kg^{-1} $(NH_4)_2SO_4$, 14.88 mol kg^{-1} NH_4NO_3] (model 1) and [2.83 mol kg^{-1} $(NH_4)_2SO_4$, 15.22 mol kg^{-1} NH_4NO_3] (the present model).

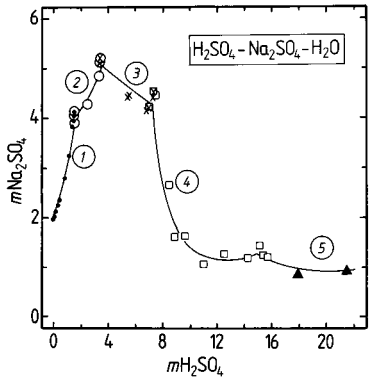

Figure 27. Salt solubilities in $H_2SO_4-Na_2SO_4-H_2O$ at 298.15 K, plotted as molalities. Data from Silcock[55] and Foote.[80] Solid phases: (1) $Na_2SO_4 \cdot 10H_2O_{(cr)}$ (dots); (2) $Na_2SO_{4(cr)}$ (open circles); (3) $Na_3H(SO_4)_{2(cr)}$ (crosses); (4) $NaHSO_4 \cdot H_2O_{(cr)}$ (open squares); (5) $NaHSO_{4(cr)}$ (solid triangles). Lines: the fitted model.

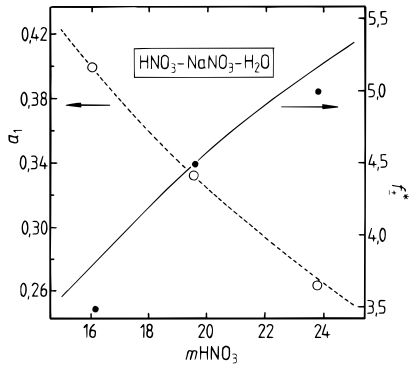

Figure 28. Water activities (a_1) and mean activity coefficients of HNO_3 ($f_\pm^*$) in $HNO_3-NaNO_3-H_2O$ at 298.15 K, plotted against HNO_3 molality. Symbols: open circles, a_1; dots, $f_\pm^*$. Lines: fitted model. Data are from vapor pressure measurements of Flatt and Benguerel.[81] The molality of $NaNO_3$ in all solutions is approximately 1 mol kg^{-1}.

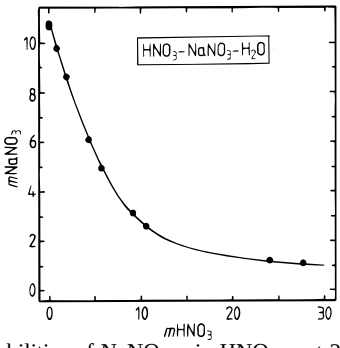

Figure 29. Solubilities of $NaNO_{3(cr)}$ in $HNO_{3(aq)}$ at 298.15 K, plotted as molalities. Symbols: data from the Gmelin Handbook[38] and Kurnakov and Nikolaev.[82] Line: fitted model.

The value of $\Delta_fG°(Na_3H(SO_4)_{2(cr)})$ obtained using the present model (−2278.9 kJ mol^{-1}) agrees to within 1 kJ mol^{-1} with the result of Harvie et al.[37] using the molality-based model of Pitzer.[8] Gibbs energies of formation of $NaHSO_4 \cdot H_2O_{(cr)}$ and $NaHSO_{4(cr)}$ differ from those listed by Wagman et al.[54] by 12.5 and 10.2 kJ mol^{-1}, respectively. These larger differences may reflect the greater uncertainties in the modeled activities for very concentrated solutions or those in the method used by Wagman et al. to obtain $\Delta_fG°$.

Salt solubilities in the quaternary systems $H^+-Na^+-SO_4^{2-}-Cl^--H_2O$ and $NH_4^+-Na^+-SO_4^{2-}-Cl^--H_2O$ have been de-

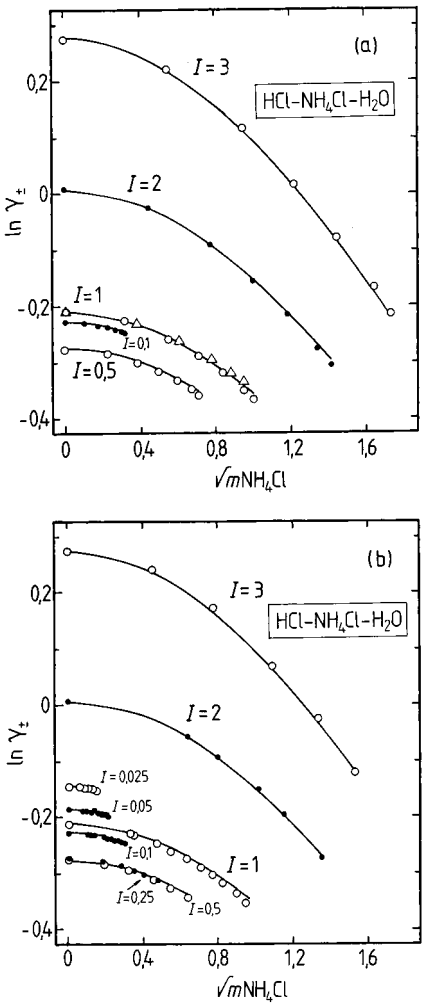

Figure 30. Mean molal activity coefficients of HCl ($\gamma_{\pm}$) in HCl−NH_4Cl−H_2O at 298.15 K, plotted against the square root of NH_4Cl molality ($m$$NH_4Cl$). Values are shown for ionic strengths (I) from 0.025 to 3.0 mol kg^{-1}. (a) Symbols: dot and open circles, Downes et al.;[41] open triangles, Chan et al.[40] Lines: fitted model. (b) Symbols: Robinson et al.[39] Lines: fitted model.

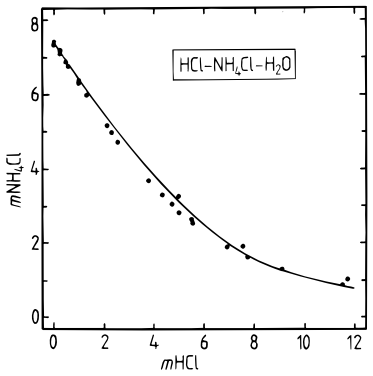

Figure 31. Solubilities of $NH_4Cl_{(cr)}$ in $HCl_{(aq)}$ at 298.15 K, plotted as molalities. Symbols: data from Silcock.[55] Line: fitted model.

termined at 298.15 K,[55] and these have been used as a test of the model. Figures 22a and 23a show measured and predicted compositions of solutions simultaneously saturated with respect to either two or three solid phases. There is excellent agreement for the NH_4^+−Na^+−SO_4^{2-}−Cl^-−H_2O system for all solid phases, over a water activity range from 0.68 to about 0.93 (Figure 22b). For the acid sulfate system the model calculated

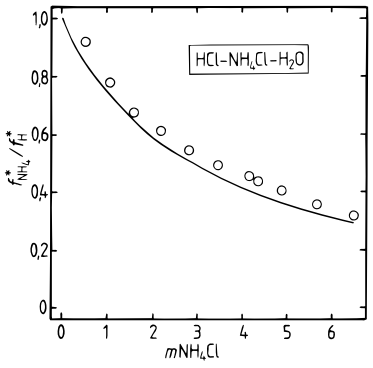

Figure 32. Reciprocal of NH_4^+ and H^+ activity coefficients in $NH_4Cl_{(aq)}$, determined from pK_a* measurements at 298.15 K. Symbols: data of Maeda et al.[42] Line: predicted by the model.

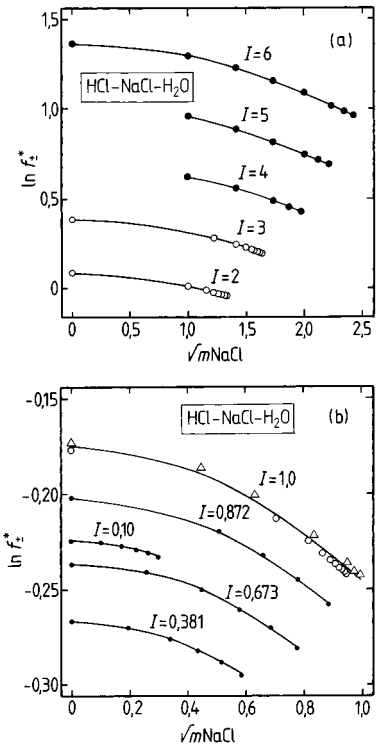

Figure 33. Mean activity coefficients of HCl ($f_{\pm}$*) in HCl−NaCl−H_2O at 298.15 K, plotted against the square root of NaCl molality (mNaCl). Values are shown for molal ionic strengths (I) marked on the plots. (a) Symbols: dots, Hawkins;[83] open circles, Harned.[84] Lines: fitted model. (b) Symbols: dots, Macaskill et al.;[44] open circles, Harned;[84] open triangles, Chan et al.[40] (1979). Lines: fitted model.

phase boundaries are also consistent with measured values, with the exception of saturation with respect to $Na_2SO_4{\cdot}10H_2O_{(cr)}$ and $Na_2SO_{4(cr)}$. However, Figure 27 shows that the model accurately predicts solubilities in the ternary system H_2SO_4−Na_2SO_4−H_2O (also for Na_2SO_4−NaCl−H_2O, Clegg et al.[17]), suggesting that the three measurements for the quaternary system which are denoted by crosses and triangles may be in error. Equilibrium water activities for the H^+−Na^+−SO_4^{2-}−Cl^-−H_2O system are shown in Figure 23b. Here the values cover a larger range, with precipitation of $Na_3H(SO_4)_{2(cr)}$ and $NaHSO_4{\cdot}H_2O_{(cr)}$ only occurring at water activities below about 0.69 and 0.53, respectively. Sodium chloride is the precipitating solid phase over most of the composition range, at water activities ranging from 0.753 (in $NaCl_{(aq)}$) to 0.41 for a cation fraction of H^+ of $\leq$0.9.

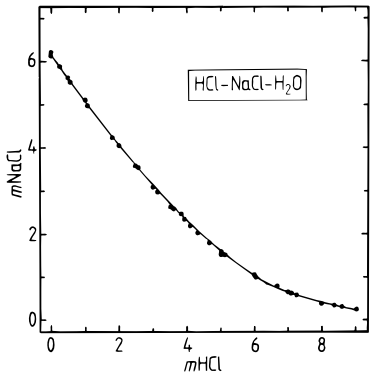

Figure 34. Solubilities of $NaCl_{(cr)}$ in $HCl_{(aq)}$ at 298.15 K, plotted as molalities. Symbols: data from Silcock.[55] Line: fitted model.

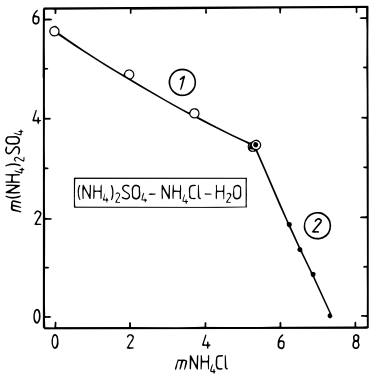

Figure 35. Salt solubilities in $(NH_4)_2SO_4-NH_4Cl-H_2O$ at 298.15 K, plotted as molalities. Data from Silcock[55] and Hill and Loucks.[85] Solid phases: (1) $(NH_4)_2SO_{4(cr)}$ (open circles); (2) $NH_4Cl_{(cr)}$ (dots). Line: fitted model.

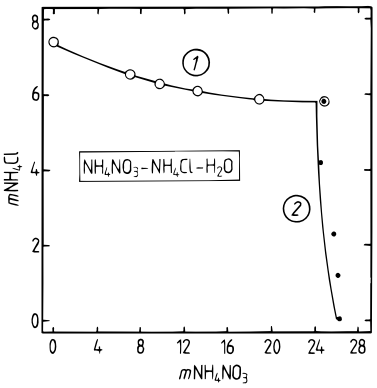

Figure 36. Salt solubilities in $NH_4NO_3-NH_4Cl-H_2O$ at 298.15 K, plotted as molalities. Data from Silcock.[55] Solid phases: (1) $NH_4Cl_{(cr)}$ (open circles); (2) $NH_4NO_{3(cr)}$ (dots). Line: fitted model.

5. Summary

The mole-fraction-based thermodynamic model presented here provides a self-consistent representation of ion and solvent activities in $H^+-NH_4^+-Na^+-SO_4^{2-}-NO_3^--Cl^--H_2O$ solutions at 298.15 K. The model has been parameterized using available vapor pressures, isopiestic and edb data, degrees of dissociation, emfs, and pK_a* measurements.

Gibbs energies of formation for 12 acid ammonium sulfate, acid sodium sulfate, and other double salts have been derived from the equilibrium constants for dissolution of the solid phases.

Comparisons with existing data for the activities required to calculate pNH_3 suggest that the model can be used to estimate this quantity with satisfactory accuracy. Comparisons with solubility measurements for quaternary solutions yield similarly good results and confirm that the model can be used to predict phase equilibria of aqueous aerosols of $H^+-NH_4^+-Na^+-SO_4^{2-}-NO_3^--Cl^--H_2O$ composition.

Note: FORTRAN code implementing the model described here is available from S. Clegg (s.clegg@uea.ac.uk) and can also be run from the following websites: http://www.uea.ac.uk/~e770/aim.html, and http://www.me.udel.edu/wexler/aim.html.

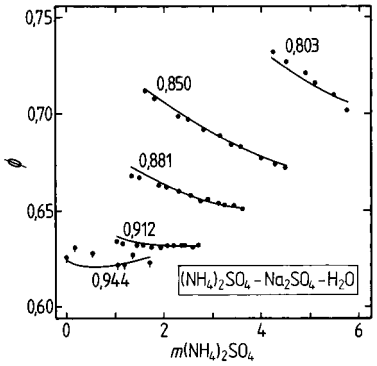

Figure 37. Molal osmotic coefficients (ϕ) of $(NH_4)_2SO_4-Na_2SO_4-H_2O$ mixtures at 298.15 K, plotted against $(NH_4)_2SO_4$ molality. Symbols: dots, data of Filippov et al.[86] Lines: fitted model. The measurements are at fixed water activities, which are indicated on the plot.

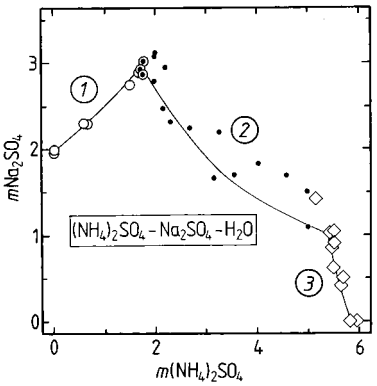

Figure 38. Salt solubilities in $(NH_4)_2SO_4-Na_2SO_4-H_2O$ at 298.15 K, plotted as molalities. Data from Silcock[55] and Sborgi et al.[87] Solid phases: (1) $Na_2SO_4 \cdot 10H_2O_{(cr)}$ (open circles); (2) $Na_2SO_4 \cdot (NH_4)_2SO_4 \cdot 4H_2O_{(cr)}$ (dots); (3) $(NH_4)_2SO_{4(cr)}$ (open diamonds). Line: fitted model.

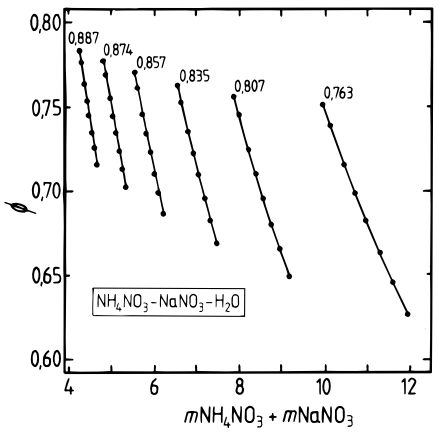

Figure 39. Molal osmotic coefficients (ϕ) of $NH_4NO_3-NaNO_3-H_2O$ mixtures at 298.15 K, plotted against total molality ($mNH_4NO_3+mNaNO_3$). Symbols: data of Kirgintsev and Lukyanov.[47] Lines: fitted model. The measurements are at fixed water activities, which are indicated on the plot.

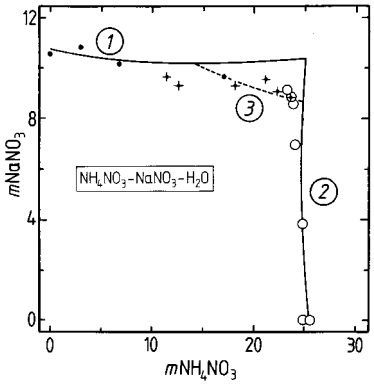

Figure 40. Salt solubilities in $NH_4NO_3-NaNO_3-H_2O$ at 298.15 K, plotted as molalities. Data from Silcock,[55] Bergman and Shulyak,[45] and Timoshenko.[46] Solid phases: (1) $NaNO3_{(cr)}$ (dots and plus symbols in principal fit of the model); (2) $NH_4NO_{3(cr)}$ (open circles); (3) $2NaNO_3 \cdot NH_4NO_{3(cr)}$ (pluses in secondary fit, with two points at lowest NH_4NO_3 molality given reduced weight). Lines: fitted model.

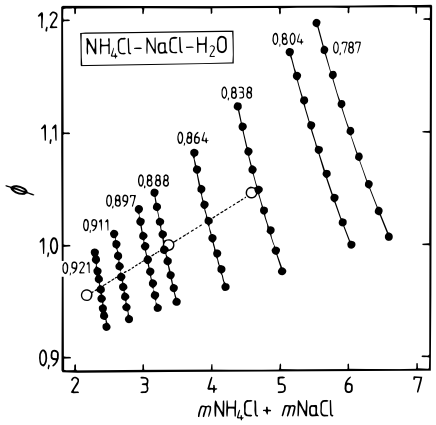

Figure 41. Molal osmotic coefficients (ϕ) of $NH_4Cl-NaCl-H_2O$ mixtures at 298.15 K, plotted against total molality. Symbols: dots, data of Kirgintsev and Lukyanov;[88] open circles, data of Maeda et al.[89] Lines: fitted model. The measurements of Kirgintsev and Lukyanov are at fixed water activities (marked on the plot), whereas those of Maeda et al. are for equimolal mixtures for $0.7907 \leq a_1 \leq 0.9281$.

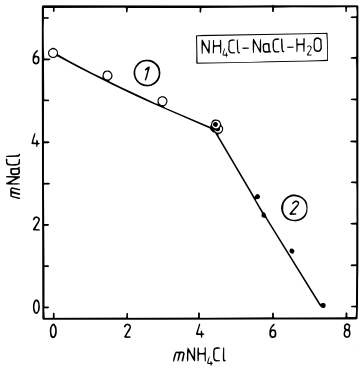

Figure 42. Salt solubilities in $NH_4Cl-NaCl-H_2O$ at 298.15 K, plotted as molalities. Data from Silcock[55] and Sborgi and Franco.[90] Solid phases: (1) $NaCl_{(cr)}$ (open circles); (2) $NH_4Cl_{(cr)}$ (dots). Line: fitted model.

Acknowledgment. This work was funded by a NATO Collaborative Research Grant (CRG 960160). We also wish to acknowledge the support of the Natural Environment Research Council (Advanced Fellowship GT5/93/AAPS/2 for S.L.C.) and a grant from the IBM Environmental Research Programme (to A.S.W.).

References and Notes

(1) Seinfeld, J. H. *Atmospheric Chemistry and Physics of Air Pollution*; John Wiley and Sons: New York, 1986.
(2) Saxena, P.; Hudischewskyj, A. B.; Seigneur, C.; Seinfeld, J. H. *Atmos. Environ.* **1986**, *20*, 1471−1484.
(3) Sangster, J.; Lenzi, F. *Can. J. Chem. Eng.* **1974**, *52*, 392−396.
(4) Pilinis, C.; Seinfeld, J. H.; Seigneur, C. *Atmos. Environ.* **1987**, *21*, 943−955.
(5) Bassett, M. E.; Seinfeld, J. H. *Atmos. Environ.* **1983**, *17*, 2237−2252.
(6) Pilinis, C.; Seinfeld, J. H. *Atmos. Environ.* **1987**, *21*, 2453−2466.
(7) Kusik, C. L.; Meissner, H. P. *AIChE J. Symp. Ser.* **1978**, *173*, 14−20.
(8) Pitzer, K. S. In *Activity Coefficients in Electrolyte Solutions*, 2nd ed.; Pitzer, K. S., Ed.; CRC Press: Boca Raton, 1991; pp 75−153.
(9) Kim, Y. P.; Seinfeld, J. H.; Saxena, P. *Aerosol Sci. Technol*. **1993**, *19*, 182−198.
(10) Clegg, S. L.; Whitfield, M. In *Activity Coefficients in Electrolyte Solutions*, 2nd ed.; Pitzer, K. S., Ed.; CRC Press: Boca Raton, 1991; pp 279−434.
(11) Pitzer, K. S.; Simonson, J. M. *J. Phys. Chem.* **1986**, *90*, 3005−3009.
(12) Clegg, S. L.; Pitzer, K. S.; Brimblecombe, P. *J. Phys. Chem.* **1992**, *96*, 9470−9479; **1994**, *98*, 1368; **1995**, *99*, 6755.
(13) Clegg, S. L.; Brimblecombe, P.; Wexler, A. S. *J. Phys. Chem.* **1998**, *102*, 2137.
(14) Carslaw, K. S.; Clegg, S. L.; Brimblecombe, P. *J. Phys. Chem.* **1995**, *99*, 11557−11574.
(15) Rood, M. J.; Shaw, M. A.; Larson, T. V. *Nature* **1989**, *337*, 537−539.
(16) Clegg, S. L.; Brimblecombe, P. *J. Aerosol Sci.* **1995**, *26*, 19−38.
(17) Clegg, S. L.; Brimblecombe, P.; Liang, Z.; Chan, C. K. *Aerosol Sci. Technol.* **1997**, *27*, 345−366.
(18) Clegg, S. L.; Brimblecombe, P. *J. Phys. Chem.* **1990**, *94*, 5369−5380; **1992**, *96*, 6854.
(19) Clegg, S. L.; Brimblecombe, P. *J. Phys. Chem.* **1989**, *93*, 7237−7248.
(20) Clegg, S. L.; Whitfield, M. *Geochim. Cosmochim. Acta* **1995**, *59*, 2403−2421.
(21) Clegg, S. L.; Brimblecombe, P. *J. Chem. Eng. Data* **1995**, *40*, 43−64.
(22) Hamer, W. J.; Wu, Y. *J. Phys. Chem. Ref. Data* **1972**, *1*, 1047−1099.
(23) Clegg, S. L.; Ho, S. S.; Chan, C. K.; Brimblecombe, P. *J. Chem. Eng. Data* **1995**, *40*, 1079−1090.
(24) Chan, C. K.; Liang, Z.; Zheng, J.; Clegg, S. L.; Brimblecombe, P. *Aerosol Sci. Technol.* **1997**, *27*, 324−344.
(25) Robinson, R. A. *J. Am. Chem. Soc.* **1935**, *57*, 1165−1168.
(26) Bezbourah, C. P.; Covington, A. K.; Robinson, R. A. *J. Chem. Thermodyn.* **1970**, *2*, 431−437.
(27) Archer, D. G. *J. Phys. Chem. Ref. Data* **1992**, *21*, 793−829.
(28) Tang, I. N.; Munkelwitz, H. R.; Wang, N. J. *Colloid Interface Sci.* **1986**, *114*, 409−416.
(29) Cohen, M. D. Ph.D. Thesis, California Institute of Technology, Pasadena, CA, 1987.
(30) Cupr, V. *Recl. Trav. Chim.* **1928**, *47*, 55−72.
(31) Coppadoro, A. *Gazz. Chim. Ital.* **1909**, *39*, 616−642.
(32) Elrod, M. J.; Koch, R. E.; Kim, J. E.; Molina, M. *J. Faraday Discuss.* **1995**, *100*, 269−278.
(33) Spann, J. F. Ph.D. Thesis, University of Arkansas, Fayetteville, 1984.
(34) Emons, H. H.; Hahn, *W. Wissenschaftl. Zeitschr.* **1970**, *12*, 129−132.
(35) Chan, C. K.; Flagan, R. C.; Seinfeld, J. H. *Atmos. Environ.* **1992**, *26A*, 1661−1673.
(36) Korf, D. M.; Shchatrovskaya, L. P. *Zh. Obshch. Khim.* **1940**, *10*, 1231−1235.
(37) Harvie, C. E.; Moller, N.; Weare, J. H. *Geochim. Cosmochim. Acta* **1984**, *48*, 723−751.
(38) *Gmelins Handbook of Inorganic Chemistry*; Verlag Chemie: Weinheim, 1966; Vol. "Sodium" (System 21).
(39) Robinson, R. A.; Roy, R. N.; Bates, R. G. *J. Solution Chem.* **1974**, *3*, 837−846.
(40) Chan, C. Y.; Khoo, K. H.; Lim, T. K. *J. Solution Chem.* **1979**, *8*, 41−52.
(41) Downes, C. J. *J. Chem. Soc., Faraday Trans.* **1975**, *1*, 425−434.
(42) Maeda, M.; Furuhashi, H.; Ikami, J. *J. Chem. Soc., Faraday Trans.* **1993**, *89*, 3371−3374.
(43) Bates, R. G.; Pinching, G. D. *J. Res. Nat. Bur. Standards* **1949**, *42*, 419−430.
(44) Macaskill, J. B.; Robinson, R. A.; Bates, R. G. *J. Solution Chem.* **1977**, *6*, 385−392.

(45) Bergman, A. G.; Shulyak, L. F. *Russ. J. Inorg. Chem.* **1972**, *17*, 593−596.
(46) Timoshenko, Yu. M. *Russ. J. Inorg. Chem.* **1986**, *31*, 1843−1844.
(47) Kirgintsev, A.; Lukyanov, A. V. *Russ. J. Phys. Chem.* **1965**, *39*, 653−655.
(48) Dingemans, P.; Dijkgraaf, L. L. *Recl. Trav. Chim.* **1948**, *67*, 225−230.
(49) Prideaux, E. B. R. *J. Chem. Soc. (Ind. Trans.)* **1920**, *39*, 182T−185T.
(50) Wu, Y. C.; Rush, R. M.; Scatchard, G. *J. Phys. Chem.* **1968**, *72*, 4048−4053.
(51) Filippov, V. K.; Cheremykh, L. M. *Vestn. Leningrad Univ. Ser. Fiz. Khim.* **1986**, *1*, 47−50.
(52) Marti, J. J.; Jefferson, A.; Cai, X. P.; Richert, C.; McMurry, P. H.; Eisele, F. *J. Geophys. Res.* **1997**, *102*, 3725−3735.
(53) Maeda, M.; Iwata, T. *J. Chem. Eng. Data* **1997**, *42*, 1216−1218.
(54) Wagman, D. D.; Evans, W. H.; Parker, V. B.; Schumm, I. H.; Bailey, S. M.; Churney, K. L.; Nuttall, R. L. *J. Phys. Chem. Ref. Data* **1982**, *11*, 1−392.
(55) Silcock, H. L. *Solubilities of Inorganic and Organic Compounds*; Pergamon: Oxford, 1979; Vol. 3.
(56) Wishaw, B. F.; Stokes, R. H. *Trans. Faraday Soc.* **1954**, *50*, 952−954.
(57) Goldberg, R. N. *J. Phys. Chem. Ref. Data* **1981**, *10*, 671−764.
(58) Clegg, S. L.; Milioto, S.; Palmer, D. A. *J. Chem. Eng. Data* **1996**, *41*, 455−467.
(59) Filippov, V. K.; Charykova, M. V.; Trofimov, Yu. M. *J. Appl. Chem. USSR* **1986**, *58*, 1807−1811.
(60) Wishaw, B. F.; Stokes, R. H. *Trans. Faraday Soc.* **1952**, *48*, 27−31.
(61) Garnsey, R.; Prue, J. E. *Faraday Trans.* **1966**, *62*, 1265−1272.
(62) Kirgintsev, A.; Luk'yanov, A. V. *Russ. J. Phys. Chem.* **1964**, *38*, 867−869.
(63) Shul'ts, M. M.; Makarov, L. L.; Yu-Jeng, S. *Russ. J. Phys. Chem.* **1962**, *36*, 1181−1183.
(64) Rard, J. A.; Miller, D. G. *J. Chem. Eng. Data* **1981**, *26*, 33−38.
(65) Indelli, A. *Ric. Sci.* **1953**, *23*, 2258−2266.
(66) Platford, R. F. *J. Chem. Eng. Data* **1973**, *18*, 215−217.
(67) Downes, C. J.; Pitzer, K. S. *J. Solution Chem.* **1976**, *5*, 389−398.
(68) Randall, M.; Scott, G. N. *J. Am. Chem. Soc.* **1927**, *49*, 647−656.
(69) Gibson, R. E.; Adams, L. H. *J. Am. Chem. Soc.* **1933**, *55*, 2679−2695.
(70) Tang, I. N.; Munkelwitz, H. R. *J. Geophys. Res.* **1994**, *99*, 18801−18808.
(71) Kirgintsev, A. N.; Luk'yanov, A. V. *Russ. J. Phys. Chem.* **1965**, *39*, 389−391.
(72) Kangro, W.; Groeneveld, A. *Z. Phys. Chem. (Neue Folge)* **1962**, *32*, 110−126.
(73) Pearce, J. N.; Hopson, H. *J. Phys. Chem.* **1937**, *41*, 535−538.
(74) Wu, Y. C.; Hamer, W. J. *J. Phys. Chem. Ref. Data* **1980**, *9*, 513−518.
(75) Rard, J. A. *J. Chem. Thermodyn.* **1989**, *21*, 539−560.
(76) Rard, J. A. *J. Chem. Thermodyn.* **1992**, *24*, 45−66.
(77) Randall, M.; Langford, C. T. *J. Am. Chem. Soc.* **1927**, *49*, 1445−1450.
(78) Harned, H. S.; Sturgis, R. D. *J. Am. Chem. Soc.* **1925**, *47*, 945−953.
(79) Covington, A. K.; Dobson, J. V.; Lord Wynne-Jones *Trans. Faraday Soc.* **1965**, *61*, 2057−2062.
(80) Foote, H. W. *Am. J. Sci. [5]* **1925**, *9*, 441−447.
(81) Flatt, R.; Benguerel, F. *Helv. Chim. Acta* **1962**, *45*, 1772−1776.
(82) Kurnakov, N. S.; Nikolaev, V. I. *Z. Phys. Chem. (Leipzig)* **1927**, *130*, 193−204.
(83) Hawkins, J. E. *J. Am. Chem. Soc.* **1932**, *54*, 4480−4487.
(84) Harned, H. S. *J. Phys. Chem.* **1959**, *63*, 1299−1302.
(85) Hill, A. E.; Loucks, C. M. *J. Am. Chem. Soc.* **1937**, *59*, 2094−2098.
(86) Filippov, V. K.; Charykova, M. V.; Trofimov, Yu. M. *Zh. Prikl. Khim.* **1987**, *60*, 257−262.
(87) Sborgi, U.; Bovalini, E.; Medici, M. *Gazz. Chim. Ital.* **1924**, *54*, 934−945.
(88) Kirgintsev, A. N.; Luk'yanov, A. V. *Russ. J. Phys. Chem.* **1963**, *37*, 1501−1502.
(89) Maeda, M.; Hisada, O.; Ito, K.; Kinjo, Y. *J. Chem. Soc., Faraday Trans. 1* **1989**, *85*, 2555−2562.
(90) Sborgi, U.; Franco, C. *Gazz. Chim. Ital.* **1921**, *51*, 1−57.
(91) Frolov, Y. G.; Nasonova, G. I. *Russ. J. Phys. Chem.* **1974**, *48*, 367−369.
(92) Liang, Z.; Chan, C. K. *Aerosol Sci. Technol.* **1997**, *26*, 255−268.
(93) Clegg, S. L.; Brimblecombe, P. *Atmos. Environ.* **1988**, *22*, 91−100.
(94) Clegg, S. L.; Brimblecombe, P. *Atmos. Environ.* **1988**, *22*, 117−129.
(95) Kotlyar-Shapirov, G. S.; Kirgintsev, A. N. *Dep. Publ. VINITI* 5609-73 **1973** (Chem. Abstr. 85:83684).
(96) Tang, I. N. *J. Geophys. Res.* **1997**, *102*, 1883−1893.
(97) Shpunt, S. Y. *Zh. Prikl. Khim.* **1946**, *19*, 293−303.